HHS Public Access

Author manuscript

J Immunol. Author manuscript; available in PMC 2024 June 15.

Published in final edited form as:

J Immunol. 2023 June 15; 210(12): 1899–1912. doi:10.4049/jimmunol.2300081.

Twist1/IRF9 interaction necessary for Interferon Stimulated Genes anti-ZIKA viral infection

Yuan You[*], **Esteban Grasso**[*,#], **Ayesha Alvero**[*], **Jennifer Condon**[*], **Tanya Dimova**[**], **Anna Hu**[*], **Jiahui Ding**[*], **Marina Alexandrova**[**], **Diana Manchorova**[**], **Violeta Dimitrova**[**], **Aihua Liao**[‡], **Gil Mor**[*,‡‡]

[*] C. S Mott Center for Human Development, Wayne State University, 275 E Hancock St, Detroit, [2]MI, 48093

[#] School of Science, University of Buenos Aires, Intendente Guiraldes 2160, Buenos Aires, 1428

[**] Institute of Biology and Immunology of Reproduction “Acad. K. Bratanov”, Bulgarian Academy of Sciences, Sofia, Bulgaria

[‡] Institute of Reproductive Health, Center for Reproductive Medicine, Tongji Medical College, Huazhong University of Science and Technology, Wuhan 430030, PR China

Abstract

An efficient immune defense against pathogens requires sufficient basal sensing mechanisms that can deliver prompt responses. Type I IFNs are protective against acute viral infections and responds to viral and bacterial infections but its efficacy depends on constitutive basal activity that promotes the expression of downstream genes known as Interferon Stimulated Genes (ISGs). Type I IFNs and ISGs are constitutively produced at low quantities and yet exert profound effects essential for numerous physiological processes beyond antiviral and antimicrobial defense, including immunomodulation, cell cycle regulation, cell survival, and cell differentiation. Although the canonical response pathway for Type I IFNs have been extensively characterized, less is known regarding the transcriptional regulation of constitutive ISGs expression. ZIKA viral infection is a major risk for human pregnancy complication and fetal development and depends on an appropriate IFNβ response. However, it is poorly understood how ZIKV, in spite of IFNβ response causes miscarriages. We have uncovered a mechanism for this function specifically in the context of early anti-viral response. Our results demonstrate that IRF9 is critical in the early response to ZIKV infection in human trophoblast. This function is contingent on IRF9 binding to Twist1. In this signaling cascade, Twist1 was not only a required partner that promotes IRF9

[‡‡] **Corresponding author:** Gil Mor, MD, PhD, gmor@med.wayne.edu, C.S. Mott Center for Human Growth and Development, Department of Obstetrics and Gynecology, Wayne State University. 275 E. Hancock St., Detroit, MI 48201 USA, Phone: 313-5771337; Fax: 313-577-8554.

Author contributions

Conceptualization, GM, YY and AL; Methodology, YY, EG, JC, TD, AH, JD, MA, DM, and VD; RNA-sequencing YY, EG, AH and JD; Writing- Original Draft, YY; Writing-Review & Editing, AA and GM; Supervision, GM and AL; Funding Acquisition, GM.

Study approval

This study was carried out in accordance with the recommendations in the Guide for the Care and Use of Laboratory Animals of the National Institutes of Health. The protocols were approved by the Institutional Animal Care and Use Committee at the Wayne State University School of Medicine (Assurance Number A3310-01).

binding to ISRE but also an upstream regulator that control basal levels of IRF9. The absence of Twist1, renders human trophoblast cells susceptible to ZIKV infection.

Keywords

IRF9; Twist1; trophoblast; Type I Interferon; Interferon beta; Zika virus

Introduction

Tissue homeostasis depends on an efficient immune defense against pathogens, which requires a sufficient baseline sensing mechanism that can deliver prompt responses (1). In addition, once the infection is cleared, mechanisms that can resolve the resulting inflammation are also required to avert chronic inflammatory conditions that can lead to tissue damage (2, 3) (4, 5)

Type I IFNs (IFNα and IFNβ) are polypeptides produced by mucosal and immune cells, as well as by infected cells, that are able to induce an anti-microbial state by modulating the innate immune response and activating the adaptive immune system (6, 7). Type I IFNs are protective against acute anti-viral infections and respond against bacterial infections but this function can have deleterious consequences as observed in autoimmune diseases (8) (9) Type I IFN responses can be induced by both viral and bacterial pathogens, which are sensed by Toll-like Receptors (TLRs), NOD-like receptors (NLRs), and RIG-I-like receptors (RLRs)(10, 11). Ligation of these receptors results in the expression of stimulator of IFN genes (STING) (12). The canonical type I IFN signaling is mediated by binding of IFNα or IFNβ to the type I Interferon associated receptors (IFNAR) leading to activation of members of the JAK kinase family (13, 14) and production of several hundred Interferon Stimulated Genes (ISGs). Activated JAK kinases phosphorylate signal transducers and activators of transcription 1 (STAT1) and STAT2 (6, 15) leading to their phosphorylation, dimerization and translocation to the nucleolus where they assemble with IFN-regulatory factor 9 (IRF9) to form a three-molecule complex called IFN stimulated gene factor 3 (ISGF3) (6, 16). ISGF3 binds to a DNA sequence known as the IFN-stimulated response element (ISRE, YAGTTTC(A/T)YTTTYCC (17)) activating the transcription of ISGs, the primary effectors of type I IFN mediated biological responses (18).

The signaling components of the canonical type I IFN pathway are ubiquitously expressed, and thus allow fast and effective responses to infections, even in the presence of low levels of IFNβ (14, 19, 20). The mechanisms regulating the basal expression of ISGs are still not clearly understood.

Trophoblast cells are the main cellular component of the placenta and, among their multiple functions, they provide immunological protection to the fetus against infections, especially viral infections (21). Trophoblast cells express Pattern Recognition Receptors (PRR), such as TLRs, Nod receptors, and RIG-1 like receptors (22), localized in the cell surface or intracellular, which allows them to detect bacterial and viral derived factors (23–28). Upon activation of TLR4 or TLR3, trophoblast cell express type I IFNβ which induces the

expression a wide range of ISGs responsible for anti-viral protection, immune regulation and cell survival (10, 29).

We and others have shown the role of placental derived IFNβ on the response to viral infections such as influenza, herpes simples virus 2 (HSV2) and Zika virus (ZIKV) (10, 28, 30). The proper regulation of the anti-viral response in the placenta is essential for the protection of the fetus and the mother (31). Excessive or dysregulated IFNβ response is responsible for fetal death or abnormal development of the fetus (10, 29, 32).

ZIKV is a mosquito-borne, positive-sense single-stranded RNA virus belonging to the family Flaviviridae (genus Flavivirus). ZIKV infection is one the best examples where infection during early pregnancy has been associated with severe congenital defects (i.e. microcephaly) and pregnancy loss (33–35). Similar as other viruses, a successful ZIKV infection of trophoblast cells is based on ZIKV capacity to inhibit Type I IFN response, an essential component of the protective antiviral response (36). The protective role of IFN-β against ZIKV has been demonstrated in IFN-β signaling-deficient mice which lack the expression of ISGs and are highly susceptible to viral infection. However, the mechanism by which ZIKV is able to escape the type I IFN response has not been elucidated.

Twist1 is a transcription factor that regulates mesenchymal differentiation and cell motility (37) and has been reported to be downregulated in miscarriages (38). Much of our understanding of Twist1 function has been associated with developmental and cancer biology, although recent reports have shown that Twist1 may also regulate immune cell function. Twist1$^{+/-}$ mice demonstrate increased pro-inflammatory cytokines, associated with increased NF-κB signaling, perinatal death, and defects in type I IFN-mediated suppression of proinflammatory cytokines in macrophages (6, 39, 40), which is suggestive of a potential role of Twist1 on type I interferon response to infections.

The objective of this study was to elucidate the molecular pathways responsible for maintaining the basal IFN response to infections and could be targeted by viral infections, such as ZIKV. Our premise was that ZIKV, by modulating the type I Interferon response, might affect trophoblast function. Using *in vitro* and *in vivo* models we identified Twist1 as a critical regulator of type I IFN signaling pathway by regulating IRF9 expression and function. Furthermore, we ascertain that Twist1 expression is inhibited as result of the anti-ZIKV response, affecting trophoblast function.

Methods

Cell Culture

Mycoplasma-free immortalized human trophoblast Sw.71 cells and human endometrial stroma cells (HESC) were cultured in DMEM/ F12 or DMEM supplemented with 10% FBS, 10 mm HEPES, 0.1 mm MEM non-essential amino acids, 1 mm sodium pyruvate, and 100 U/ml penicillin/streptomycin (Life Technologies; Waltham, MA, USA) under 5% CO2 at 37°C.

Viral infections were done as previously described (41, 42).In short, cells were seeded in 6-well plates at 1.5×10^5 cells per well; the next day, ZIKV was added to the cells for 1 h incubation (at indicated MOI) with gentle agitation every 20 min, and after 1 h, the inoculum was removed, and the cells were washed twice with phosphate-buffered saline (PBS) and then cells were maintained in 10% FBS DMEM/F12 media for the duration of the experiment. At indicated time points after infection, cell pellets and conditioned media were collected for downstream analysis.

Formation of Blastocyst-Like Spheroids

BLS were obtained as previously described (43, 44), In brief, first trimester trophoblast Sw.71 cells were trypsinized and then 4,000 of these cells were added to each well of a Costar ultra-low attachment 96-well microplate (Corning Incorporated, Corning, NY, USA). Cells were incubated for 48 hr until achieved a compact morphology (spheroid). Morphology was monitored using the IncuCyte Zoom (Essen Biosciences, Ann Arbor, MI, USA). The differential cellular characteristics of trophoblast cells as a 3D model or monolayer are described in detail elsewhere (45).

Knockout of Twist1 using CRISPR/Cas9

Twist1 was knocked out in Sw.71 first-trimester trophoblast cell line using CRISPR/Cas9. The guide RNA for ISG20 was designed using the CRISPR design tool from the Zhang Laboratory at MIT (CRISPR.mit.edu) (46). Two DNA oligos were synthesized as follows: sense: 5′-TAGGCGGGAGTCCGCAGTCTTACG-3′ and antisense: 5′-AAACCGTAAGACTGCGGACTCCCG-3′. Oligos were phosphorylated using T4 polynucleotide kinase and annealed by heating equimolar amounts to 95°C and cooling slowly to room temperature. This resulting guide was introduced to lentiCRISPRv2GFP plasmid using BsmBI restriction sites, and lentiCRISPRv2GFP was a gift from David Feldser (Addgene plasmid # 82416) (47). 10 μg of the resulting plasmid was co-transfected with 8 μg of packaging plasmid pCMV-VSV-G and 4 μg of envelope plasmid psPAX2 in the presence of 60 μg of polyethylenimine (PEI) into HEK293T cells in a 100-mm dish. pCMV-VSV-G was a gift from Bob Weinberg (Addgene plasmid # 8454) (48), and psPAX2 was a gift from Didier Trono (Addgene plasmid # 12260). Then, packaged viral particles were collected by ultracentrifugation and were transduced into the Sw.71 cells. The cells were sorted based on the. The deletion of Twist1was confirmed using Sanger sequencing technique performed by GENEWIZ, and the overall efficiency was 91.1% analyzed by TIDE (Tracking of Indels by Decomposition). Protein expression was verify by Western blot.

Placenta Samples

All human samples used in this study were obtained in accordance with the guidelines of The Declaration of Helsinki and approved by Human Research Ethics Committee at the University Obstetrics and Gynecology Hospital “Maichin Dom”, Medical University, Sofia, Bulgaria (No 250569/2018). Written informed consent was taken from all women. Healthy pregnant women in early pregnancy, directed to elective pregnancy termination (6–12 gw, n = 20) were involved in the study. Pregnancies complicated by clinical evidence of infection, steroid treatment, AIDS, alcohol abuse, and/or drug abuse and immune-associated diseases

were excluded. Chorion samples were collected in sterile phosphate-buffered saline (PBS) and processed within 1 hour.

Histology and immunohistochemistry (IHC)

Early pregnancy trophoblast tissues (10 mm × 10 mm × 10 mm) were fixed in formalin-free HOPE fixative acc. to the manufacture's recommendations (Innovative Diagnostik-System, Hamburg, Germany) and embedded in paraffin wax. The paraffin sections (5 μm) were routinely stained with hematoxylin/eosin for histological investigation and then selected slides were subjected to IHC for Twist staining using three-step biotin–streptavidin enzyme method.

Tissue sections were deparaffinized and rehydrated through graded alcohol. Endogenous peroxidase activity was quenched by incubation in 3% hydrogen peroxide for 30 minutes at 37°C. To suppress nonspecific background staining the sections were blocked with Super Block (SkyTec Laboratories). Rabbit anti-human polyclonal antibody against Twist1 (25465–1-AP, Proteintech) was applied to the sections for overnight incubation at 4°C in a humidified chamber. Then the sections were processed with UltraTek Anti-Polyvalent visualization system (SkyTec Laboratories, Logan, UT, USA) according to the SkyTek kit protocol. The endogenous biotin was blocked with Biotin blocking kit (SkyTec Laboratories, Logan, UT, USA). The peroxidase activity was revealed with ready-to-use 3,3-diaminobenzidine tetrahydrochloride (DAB). Nuclei were slightly counterstained with hematoxylin. Between the incubations the slides were washed in PBS. Negative staining controls were performed by omitting of first antibody. Sections from human breast cancer tissue processed in the same way were used as positive controls for specificity of Twist staining.

Immunocytochemistry (ICC)

Sw71 and Sw71-Tw-KO cells as monolayer and spheroids were used in this study. The characterization of these cells has been reported in numerous publications (49–51).

3D Sw71 models or 2D Sw71 monolayers were cultured for 24–48 hrs in sterile culture chambers on a glass slide (Falcon). The cells were fixed in 2% paraformaldehyde (PFA) in PBS, overnight (ON) at RT and stained for HLA-G and HLA-C using indirect immunofluorescent method. After washing with PBS, the cells were incubated with Super Block (SkyTec Laboratories, Logan, UT, USA) to suppress the non-specific binding. As primary antibodies we used anti-human rabbit polyclonal antibodies against HLA-G (E-AB-18031, Elabscience) and HLA-C (E-AB-17922, Elabscience) in appropriate dilutions for overnight incubation at 4°C. As a secondary antibody goat anti-rabbit IgG conjugated with AF488 (E-AB-1055, Elabscience) was applied. Negative controls were prepared by omitting primary antibody and/or secondary antibody.

Luminex Multiplex Assay

For In vivo study, mice serum samples were collected as previously described (41). Supernatants were collected from cell cultures, centrifuged, aliquoted, and stored until use. The samples were thawed only once immediately prior to running the assay. The samples

were run on the Luminex Multiplex Assay (R&D Systems, Minneapolis, MN) as previously described (52) for the following cytokines and chemokines: IL-1α, IL-1β, IL-2, IL-3, IL-4, IL-5, IL-6, IL-9, IL-10, IL-12 (p40), IL-12 (p70), IL-13, IL-17A, Eotaxin, G-CSF, GM-CSF, IFN-γ, KC, MCP-1 (MCAF), MIP-1α, MIP-1β, RANTES, TNF-α.

RNA Isolation and Quantitative RT-PCR Analysis

Total RNA was harvested from Sw71 cells or TWKO cells using the QIAGEN RNeasy mini kit and RNase-Free DNase Kit (Qiagen, Valencia, CA, USA) according to the manufacturer's protocol. RNA samples were quantified using the Nanodrop One spectrophotometer (ThermoFisher). The purity of the RNA was assessed through the A260/A280 and A260/A230 levels. Individual mRNA abundance was determined using TaqMan one-step RT-PCR procedures on the CFX Connect Real-Time System (Bio-Rad Laboratories). Primer-probe sets for TaqMan assays were purchased from Applied Biosystems (ThermoFisher). Relative expression values for each gene were calculated using a standard curve and the reference gene peptidylprolyl-isomerase B (PPIB). Transcript levels of specific cytokines and chemokines were measured in Sw71 treated for 6 hr with IFNβ. Assay data was analyzed using the delta-delta Ct method with Bio-Rad CFX Manager 3.1 software.

RNA Sequencing

RNA sequencing service was performed by GENEWIZ. Total RNA from Sw71 and TWKO cells were extracted using Qiagen RNeasy Mini kit following manufacturer's instructions (Qiagen, Hilden, Germany) and quantified using Qubit 2.0 Fluorometer (ThermoFisher Scientific, Waltham, MA, USA) and RNA integrity was checked using TapeStation (Agilent Technologies, Palo Alto, CA, USA). The RNA sequencing library was prepared using the NEBNext Ultra II RNA Library Prep Kit for Illumina using manufacturer's instructions (New England Biolabs, Ipswich, MA, USA). Briefly, mRNAs were initially enriched with Oligod(T) beads. Enriched mRNAs were fragmented for 15 minutes at 94 °C. First strand and second strand cDNA were subsequently synthesized. cDNA fragments were end repaired and adenylated at 3'ends, and universal adapters were ligated to cDNA fragments, followed by index addition and library enrichment by PCR with limited cycles. The sequencing library was validated on the Agilent TapeStation (Agilent Technologies, Palo Alto, CA, USA), and quantified by using Qubit 2.0 Fluorometer (ThermoFisher Scientific, Waltham, MA, USA) as well as by quantitative PCR (KAPA Biosystems, Wilmington, MA, USA).

Sequencing: The sequencing libraries were multiplexed and clustered onto a flowcell. After clustering, the flowcell was loaded onto the Illumina HiSeq instrument according to manufacturer's instructions. The samples were sequenced using a 2×150bp Paired End (PE) configuration. Image analysis and base calling were conducted by the HiSeq Control Software (HCS). Raw sequence data (.bcl files) generated from Illumina HiSeq was converted into fastq files and de-multiplexed using Illumina bcl2fastq 2.17 software. One mis-match was allowed for index sequence identification. After investigating the quality of the raw data, sequence reads were trimmed to remove possible adapter sequences and nucleotides with poor quality using Trimmomatic v.0.36. The trimmed reads were mapped to

the [SPECIES] reference genome available on ENSEMBL using the STAR aligner v.2.5.2b. BAM files were generated because of this step. Unique gene hit counts were calculated by using feature Counts from the Subread package v.1.5.2. Only unique reads that fell within exon regions were counted. After extraction of gene hit counts, the gene hit counts table was used for downstream differential expression analysis. Using DESeq2, a comparison of gene expression between the groups of samples was performed. The Wald test was used to generate P values and Log2 fold changes. Genes with adjusted P values < 0.05 and absolute log2 fold changes >1 were called as differentially expressed genes for each comparison. Gene ontology analysis was performed on the statistically significant set of genes by implementing the software GeneSCF. The goa_[SPECIES] GO list was used to cluster the set of genes based on their biological process and determine their statistical significance.

Bioinformatic analysis:

Differential expression analysis was performed in R using the Linear Modeling for MicroArray (LIMMA) package (53, 54). Linear models were fitted to the protein abundance matrix with fetal sex, mother identity, and treatment considered as covariates. LIMMA implements empirical Bayes-based moderated t-statistic for significance analysis. For each experimental pair contrasted, proteins were considered differentially expressed if the corresponding p-value was < 0.05 and log2 fold change >0.6. Gene Ontology and Pathway analyses were performed using the iPathwayGuide software from AdvaitaBio (55–58). Gene Ontology terms and KEGG pathways were considered significantly enriched if the respective FDR-adjusted p-values was < 0.05. PCA plots were generated using the pcaExplorer package (59), heatmaps were generated using the ComplexHeatmap package (60), enriched gene ontology terms and pathways were graphed using the ggplot2 package (61) in R. The GOplot package was used to generate chord plots of the shown enriched Gene Ontology terms and constituent genes.

Luciferase assay

Sw71 WT or TW-KO cells were transfected with the ISRE (Interferon Stimulated Response Element) reporter kit plasmids (BPS Bioscience, USA, cat#60613) or co-transfected with either WT Twist1 plasmid or different Twist1 mutants in 96 well plate using FuGENE® 6 Transfection Reagent (Promega, USA, Cat.# E2691) according to manufacture protocol. After transfection, the cells are incubated in culture medium for 24 hours to allow for expression of the luciferase gene.

Statistics

Statistical analyses were performed using Prism software, version 8 (GraphPad, San Diego, CA). All data are presented as means ± SEM. For mouse studies, a mixed model ANOVA was utilized. When appropriate (when significance of a factor or of interaction was established by the initial analysis), an analysis of simple effect was performed using one-way ANOVA as needed. As needed, differences, between two groups were analyzed using unpaired Student's *t*-test and differences among multiple groups were analyzed by one-way ANOVA. Depending on the distribution of the continuous variables, nonparametric

test was used if the data was not normally distributed. A p-value < 0.05 was considered statistically significant.

Results

ZIKV infection inhibits trophoblast migration

The migration of trophoblast cells from the trophectoderm and subsequent invasion towards the endometrial stroma are critical steps in embryo implantation (62, 63). We questioned whether ZIKV infection could affect these processes. Thus, we utilized a previously reported *in vitro* system of 3D blastocyst-like structures (BLS) formed from first trimester Swan71 trophoblast cells (43) (Fig. 1A). Under normal culture conditions, transfer of BLS from ultra-low attachment conditions to tissue-culture treated wells showed attachment within 24h and migration of trophoblast cells from the BLS (Fig. 1B–C). However, pre-treatment with ZIKV for 24h prior to the transfer, prevented BLS attachment and significantly inhibited trophoblast migration (Fig. 1B–E). These results shown that ZIKV infection can prevent successful attachment and migration of BLS *in vitro*.

Twist1 expression in placenta and trophoblast cells

Migration and invasion are accomplished by cells with mesenchymal phenotype. Twist1 is a transcription factor and master regulator of epithelial-mesenchymal transition (37) and has been reported to be downregulated in miscarriages (38). The Human Protein ATLAS (https://www.proteinatlas.org/ENSG00000122691-TWIST1/tissue) showed that Twist1 is highly expressed in the placenta and endometrium (Fig 2A). Thus, we stained first trimester human placentas to determine Twist1 cellular expression and observed cell-specific expression in extravillous trophoblast (EVT) but not the villi syncytio and cytotrophoblast (Fig. 2B). Twist1-positive EVT cells can be observed in the decidua and in close proximity to Twist1-negative decidual cells and immune cells (Fig. 2Ci–ii). We also identified Twist1-positive trophoblast cells within the glandular epithelium (Fig. 2Ciii). Interestingly, EVT cells in placental samples from miscarriages showed lower Twist1 expression compared to first trimester normal placenta. (Fig 2D).

We then evaluated Twist1 expression in monolayer cultures of established first-trimester trophoblast cell lines (Swan71 and 3A) and primary cultures of villi-derived first trimester trophoblast (AL06 and AL07). We also evaluated Twist1 expression in the Swan71 BLS. Similar to the findings in the placenta, AL06, AL07 and 3A showed no Twist1 expression; on the other hand, Swan71 and its derived BLS, which express mesenchymal phenotype (43), were positive for Twist1 (Fig. 3A). Since EVTs are the trophoblast cells with migratory capacity, the specific expression of Twist1 in these cells further support the role of Twist1 in trophoblast migration and invasion.

Mouse models are instrumental in increasing our knowledge of extra-embryonic development, and although there are differences between human and mouse placentation, it still is a practical and accessible model to monitor the developmental process. Thus, we determined whether Twist1 expression is associated with the development of mouse placenta. We collected placental samples throughout gestation starting at Embryonic Day

(E) 8.5 (when placenta tissue is available) until E18.5 and examined Twist1 expression by western blot. As shown in figure 3B, Twist1 expression is detectable in the mouse placenta although its expression varied along the gestation. We observed the highest expression around E8.5-E10.5 and lower expression in latter times (Fig 3B–C). The high level of Twist1 during the E8.5-E10.5 period corelates with the process of trophoblast invasion and formation of the labyrinth which takes place in the mouse around this period (64, 65).

Cellular inflammatory response against viral signals inhibits Twist1 expression

Since we saw that ZIKV infection inhibits trophoblast migration, we examined whether it can affect Twist1 expression. Thus, Swan71 trophoblast cells were infected with ZIKV (Cambodia and Brazil strains) for 1h and samples were collected 48h post infection (p.i). Our data showed that infection with both ZIKV strains downregulated Twist1 expression both at the mRNA (Fig 4A) and protein level (Fig 4B).

To distinguish whether the inhibition of Twist1 is a direct result of ZIKV or a result of a cellular anti-viral response due to the infection, we treated Swan71 trophoblast cells with Poly IC, a synthetic polyinosinic-polycytidylic acid double-stranded RNA for 24h. Similar to the results observed with ZIKV infection, Poly IC treatment inhibited Twist1 protein expression *in vitro* (Fig 3C). To determine if this response also occurs *in vivo*, pregnant mice were treated with Poly IC at E8.5 (20 μg/kg). We saw the induction of pregnancy loss in poly IC-treated mice within 24h post treatment (Fig. 4D–E) and analysis of placental samples at an earlier time point (4 hours post poly IC) showed decrease in Twist1 expression. Taken together, these findings suggest that the anti-viral response elicited from the trophoblast and not the ZIKV itself may be the regulatory mechanism that downregulates Twist1.

Interferon Beta inhibits Twist1 expression and trophoblast migration.

A common cellular response to ZIKV infection and Poly IC treatment is the expression of Type I IFNβ (Fig. 5A–B and (66)). *In vitro*, we saw increased levels of IFNβ in Swan71 trophoblast cells following ZIKV infection (Fig. 5A), and *in vivo*, we can detect high levels of IFNβ in the serum of Poly IC treated pregnant mice (Fig. 5B). We posit that cellular IFNβ, produced in response to viral infection, could be responsible for the decrease on Twist1 expression in the trophoblast. To test this hypothesis, we treated Swan71 trophoblast cells with IFNβ (30 ng/ml, 24h). Detection of Twist1 mRNA by qPCR showed that IFNβ treatment downregulates Twist1 mRNA expression (Fig. 5C). The decrease in Twist1 was validated at the protein level. Treatment of Swan71 trophoblast cells for 24h with 3 or 30 ng/ml IFNβ showed a dose-dependent decrease in Twist1 expression. Moreover, treatment of Swan71 trophoblast cells with 30 ng/ml IFNβ for 2, 8 16 and 24 hours showed an initial increase in Twist1 expression at the early 2h time point followed by a time-dependent decrease in Twist1 protein expression in the succeeding time points (Supp. Fig. 1). The inhibitory effect of IFNβ on Twist1 is restricted to Twist1 since we observed increased expression of other ISGs such as Viperin, IFITM or ISG15 (Supp. Fig 2).

To confirm the link between IFNβ-induced inhibition of Twist1 and trophoblast migration, we treated Swan71 BLS with increasing concentrations of IFNβ (3, 30 ng/ml) and

monitored trophoblast attachment and migration by live imaging. As described above, BLS attached to the plate within 24 hours followed by trophoblast migration; however, in the presence of IFNβ, trophoblast attachment and migration were significantly inhibited (Fig. 5E). These results demonstrate that IFNβ exerts a major regulatory role in Twist1 expression and migration in trophoblast cells.

Twist1 is required for trophoblast migration and successful anti-viral response

To further demonstrate the role of Twist1 in trophoblast cell migration and response to viral infection, we knocked-out Twist1 in Swan71 trophoblast cells using CRISPR/Cas9 and generated a Twist1-KO clone (Swan71 TW-KO) (Fig 6A). The specific sequence deleted on the Twist1 gene is shown in figure 6B. TW-KO cells were able to form BLS, however these cells lost the capacity to migrate and invade (Fig 6C–D) demonstrating the requirement of Twist1 in trophoblast migration and invasion.

To determine the role of Twist1 in response to viral infection, monolayer cultures of wild-type (WT) Swan71 trophoblast cells and Swan71 TW-KO cells were infected with ZIKV. Surprisingly, we observed a significant increase in ZIKV titers in Swan71 TW-KO cells compared to WT Swan71 trophoblast cells (Fig. 7A). Furthermore, Swan71 TW-KO cells are more sensitive to ZIKV infection and undergo cell death 48 hours post infection (Fig 7B). In contrast, WT Swan71 maintained cell viability when infected with ZIKV (Fig 7B).

Trophoblast cells control ZIKV infection through the expression of antiviral ISGs, such as ISG20, Mx1, ISG15 and Viperin, which can impede distinct steps in the viral cycle (10). As shown in Figure 7C, ZIKV infection in WT Swan71 trophoblast cells triggers the expression of these ISGs; however, this response was significantly dampened in the Swan71 TW-KO cells (Fig. 7C).

To conclusively demonstrate the role of Twist1 in the cellular anti-viral response we overexpressed Twist1 in Swan71 TW-KO followed by infection with ZIKV. The overexpression of Twist1 significantly decreased viral copy numbers compared to Swan71 TW-KO cells and was able to restore both the basal and anti-viral levels of ISG20, Mx1 and Viperin (Fig. 7D–E). These findings demonstrate that Twist1 is not only necessary for trophoblast migration but also has an impact on the expression of anti-viral ISGs necessary to control ZIKV infection.

Twist1 regulates basal levels of IRF9

To identify specific pathways and cellular processes regulated by Twist1 in trophoblast cells, we compared the transcriptome of WT Swan71 trophoblast cells and Swan71 TW-KO cells. We observed 644 upregulated genes and 1140 downregulated genes in the Swan71 TW-KO cells compared to the WT Swan71 trophoblast cells (Fig. 8A). Dendrogram analysis of differentially regulated biological processes using high-specificity pruning showed differential regulation of extracellular matrix organization, which explains the observed effect on trophoblast migration and invasion. More importantly, we observed that several processes related to viral response such as type I interferon signaling pathway, negative regulation of viral genome replication and defense response to viral infections were also differentially regulated in Swan71 TW-KO cells compared to WT Swan71 trophoblast cells

(Fig 8B). A closer analysis of differentially expressed genes (DEGs) in the type I interferon signaling pathway showed that majority of ISGs (Mx1, Mx2, XAF1, ISG15, ISG20 and IRF9) were downregulated in Swan71 TW-KO cells compared to WT Swan71 trophoblast cells (Fig. 8C). Network analysis of DEGs in the type I interferon signaling pathway showed IRF9 as the central regulator of this pathway downstream of Twist1 (Fig 8D). The downregulation of IRF9 in Swan71 TW-KO cells was validated both at the protein level in total cell lysate (Fig. 9A) as well as on its cytoplasmic and nuclear fraction (Fig 9B). Similarly, we observed a significant decrease on the basal levels of ISG20, ISG15, Mx1 and Viperin (Fig. 9C). Noteworthy, non-classical Human Leukocytes antigens (HLA) G, C and F were also identified as significantly downregulated in Swan71 TW-KO cells compared to WT Swan71 trophoblast cells in the transcriptomic analysis (Fig. 8C). HLA-G and C are expressed in EVTs and have immune suppressive function on immune cells, particularly NK cells (67, 68). Immunofluorescence analysis for HLA-G confirmed its basal expression in WT Swan71 trophoblast cells and decreased expression in Swan71 TW-KO cells (Fig. 9D). Taken together these findings demonstrate that Twist1 expression has an impact on ISGs expression in trophoblast cells.

Next, we sought to identify the specific mechanism by which Twist1 regulates the type I IFN signaling pathway in response to viral infection. We first determined changes in the expression of IFNβ or its receptor following ZIKV infection but did not observe any differences in the levels of IFNβ ligand and the IFNAR1 receptor between WT Swan71 trophoblast cells and Swan71 TW-KO cells both at baseline and with ZIKV (Supp. Fig. 3), demonstrating that the recognition of the virus and the production of IFNβ is Twist1-independent. We then evaluated the propagation of the signaling pathway downstream of IFNβ signaling (Fig. 10A). Thus, WT Swan71 trophoblast cells and Swan71 TW-KO cells were treated with IFNβ (30 ng/ml) for 2h and levels of phosphorylated-STAT1 (pSTAT1) and phosphorylated-STAT2 (pSTAT2), which are the two main mediators of the canonical IFNβ signaling pathway(69), were determined by western blot. We saw the upregulation of pSTAT1 and pSTAT2 in both the WT Swan71 trophoblast cells and Swan71 TW-KO cells (Fig. 10B). The increase on pSTAT1 and pSTAT2 following IFNβ treatment was time dependent, peaking approximately around 16h post IFNβ treatment (Supp. Fig. 1) in both the WT Swan71 trophoblast cells and Swan71 TW-KO cells. We did not observe the presence of pSTAT1 or pSTAT2 in the control group, neither the wt or KO cells (Supp. Fig. 1). These findings suggest that the effect of Twist1 on the IFNβ signaling pathway is downstream of STAT phosphorylation.

As stated above, IRF9 was down-regulated in Swan71 TW-KO cells compared to WT Swan71 trophoblast cells, in the cytoplasm as well as in the nucleus (Fig. 9B) and Twist1 is mainly expressed in the nucleus in WT Swant71 cells but is not detected in the KO cells (Fig. 9B). The lower levels of IRF9 in the Swan71 TW-KO cells, however, did not affect the nuclear translocation of pSTAT1 and pSTAT2 upon INFβ treatment (Fig. 10C). However, analysis of ISGs, which are more downstream in the pathway, showed that only the WT Swan71 trophoblast cells and not Swan71 TW-KO cells were able to upregulate the ISGs Mx1 and ISG20 in response to IFN treatment (Fig. 10B). Taken together, these results demonstrate that the critical node controlled by Twist1 in the IFNβ pathway is the basal level of IRF9.

Protein-Protein interaction between Twist1 and IRF9

We then determined if overexpression of IRF9 in Swan71 TW-KO cells will be sufficient to restore the capacity to control ZIKV replication. Thus, Swan71 TW-KO cells were stable transfected with pIRF9OE plasmid and infected with ZIKV. Despite the successful overexpression of IRF9 (Fig. 10D) and in contrast to the overexpression of Twist1, these cells were not able to control ZIKV replication any better than Swan71 TW-KO cells (Fig. 7D).

We further tested whether Twist1 can modulate IRF9 interaction with the ISRE by using an ISRE luciferase reporter system. This reporter contains a firefly luciferase gene under the control of multimerized ISRE responsive elements located upstream of a minimal promoter. The ISRE reporter is premixed with constitutively-expressing renilla luciferase vector, which serves as an internal control for transfection efficiency (Supp. Fig. 4).

Transfection of the ISRE luciferase reporter system in WT Swan71 trophoblast cells showed luciferase activity, which was significantly downregulated in Swan71 TW-KO cells (Fig. 11A). Interestingly, overexpression of IRF9 alone or Twist1 alone in Swan71 TW-KO cells did not rescue the luciferase activity on the ISRE (Fig. 11A). Conversely, co-expression of Twist1 and IRF9 in Swan71 TW-KO cells was able to rescue luciferase activity in the ISRE similar to the levels observed in WT Swan71 trophoblast cells (Fig. 11A). These results indicate that, without Twist1, IRF9 is not enough to control ZIKV infection. These findings place Twist1as part of IRF9 protein complex necessary for an early antiviral response.

Twist1 can directly bind the DNA at conserved E-box motif or other transcriptional regulators and control their actions on the promoter. To determine whether the regulatory role of Twist1 in the ISRE depends on its interaction with the DNA, we used several constructs of Twist1 with specific deletions and tested their effect on ISRE luciferase reporter system (Fig. 11B). We first tested ΔHLH construct, which has deletion in the DNA binding domain and compared its effect on ISRE reporter with full length Twist1. As shown above, co-transfection of IRF9 with full-length Twist1 rescued luciferase activity in the ISRE. Interestingly, co-transfection of IRF9 with ΔHLH in Swan71 TW-KO cells was also able to rescue the activity of luciferase on the ISRE reporter (Fig. 11C). Since the reporter system does not contain an E-box sequence, these results demonstrate that direct binding to the E-box is not required for Twist1 to regulate ISG levels and suggest that protein-protein interaction may be the mechanism by which Twist1 regulates ISGs.

To test this hypothesis, we co-transfected IRF9 with Δ29–119, Δ51–82 and ΔWR, which are constructs with deletions in the Twist1 domains necessary for interaction with other proteins. Deletion of these domains failed to rescue the activity of luciferase on the ISRE reporter (Fig. C). Given that these domains are important for protein-protein interaction, these results further suggest that Twist1-IRF9 protein interaction is necessary for Twist1's activity on the ISRE

To further validate this hypothesis, we overexpressed both myc-tagged Twist1 and Flag-tagged IRF9 and performed immunoprecipitation to determine if Twist1 binds IRF9. First, we immunoprecipitated myc and immunoblotted for IRF9. Analysis of the isolated

immunocomplex demonstrated the presence of IRF9 (Fig. 11D). Similarly, when we IP Flag and blotted for Twist1, we observed Twist1 in the isolated immunocomplex (Fig. 11D), further confirming that Twist1 binds IRF9. We did not detect the presence of pSTAT1 or pSTAT2 in the IP complex (Supp. Fig. 4B). Taken together, our results demonstrate that Twist1, by binding to IRF9, is able to control IRF9 basal expression; a step necessary for the response to ZIKV infection.

Discussion

Our study uncovered the mechanisms by which Twsit1-IRF9 complex is able to provide an early anti-viral response. IRF9 is a transcription factor that mediates the Type I IFN response (6, 70). Ligation of IFNAR by Type I IFNs results in the phosphorylation and dimerization of STAT1 and STAT2 (70). This dimer then recruits IRF9 to form the ISGF3 complex in cytoplasm. ISGF3 then translocate to the nucleus and binds to the ISRE leading to the transcription of ISGs (71). IRF9 has also been shown to regulate cell proliferation (70), tumor formation (72), cardiovascular disease (73), inflammation (74), and immune cell regulation (75) independent of the ISGF3 complex. However, the mechanisms that allow IRF9 to function outside of the ISGF3 complex is not well understood. Our data provides a novel model where IRF9 in conjunction with Twist1 provides a continue and effective basal protection. However, upon recognition of viral factors by PRR, IFNβ expression is induced and activates the IFNAR pathway which promotes Twist1 dissociation from the IRF9 complex allowing the strong response mediated by the most efficient ISGF3 complex (Fig. 12).

We have uncovered a mechanism for this function specifically in the context of early anti-viral response. Our results demonstrate that Twist1 was not only a required partner that promotes IRF9 binding to ISRE but also an upstream regulator that control basal levels of IRF9. Deletion of Twist1 decreases IRF9 mRNA and other ISGs, impairing the initial anti-viral response on infected cells.

Interestingly, although the loss of Twist1 lead to decreased basal IRF9 and ISG levels, it did not affect canonical response to Type I IFN. In Twist1 deficient cells, IFNβ maintained the ability to lead to phosphorylation of STAT1 and STAT2, to promote nuclear translocation of ISGF3, and to induce a significant increase on ISGs expression. Consequently, we postulate that Twist1 is an additional mechanism necessary to maintain the basal expression of IRF9/ISGs in the absence type I IFN or in the presence of low levels of IFNβ.

Basal expression of IRF9 and ISGs are essential to maintain a state of “readiness” to combat infection. By itself, IRF9 has low affinity to ISREs and therefore requires additional transcriptional factors to improve DNA binding (76, 77) and transcriptional activity (70). Our data demonstrate that Twist1 promotes IRF9 binding to DNA.

IRF9-Twist1 binding requires an intact C-terminal component of Twist1. Deletion of the WR domain but not the HLH domain (DNA binding domain) of Twist1 inhibited the capacity to bind IRF9 and to enhance ISRE activity. Based on these findings we postulate that Twist1 interacts with IRF9 in the nucleus and increases IRF9 transcriptional efficacy for ISRE

regulated genes. This interaction ensures the basal expression of ISGs, which is essential for the early protection against viral infections.

The importance of this basal expression is exemplified during viral infections such as ZIKV. Viral infections during pregnancy can have various outcomes ranging from no consequence to spontaneous abortion or successful birth but with associated congenital viral syndromes (30, 78–80). The outcome seems to be dictated by the gestational timing of the infections with early infections being associated with pregnancy loss and fetal demise (81–83).

The placenta is an extraembryonic organ that ensures appropriate supply of nutrients and oxygen to the fetus. In addition to this, it provides immunological protection and, as such, is a critical regulator of fetal growth and development. The formation of the placenta takes place during the early stages of embryo implantation and is the result of the migration of trophoblast cells from the trophectoderm and its invasion into the maternal endometrial/decidual tissue. The process of trophoblast migration and invasion is essential for the success of the pregnancy and is supported by maternal factors produced by decidual cells (84, 85). There are many ethical challenges in the study of human implantation but the use of *in vitro* models that mimic the biological components of human implantation has overcome some of these limitations. In this study we used a well characterized model that mimics, with its obvious limitations, the capacity of human trophoblast to migrate and invade (43, 44) and we showed that ZIKV infection perturbs trophoblast migration. We postulate that by affecting trophoblast migration, ZIKV infection during early pregnancy may lead to miscarriage. Indeed, pregnancy loss in women change as gestational age advances, with a rate of ~25% at 4–5 weeks, 2% at 20 weeks and 0.1% after 20 weeks' gestation (86). In cases infected with ZIKV, it was reported that 5.8% miscarriage rate and a 1.6% stillbirth rate occur when the women are infected during the first trimester (87).

Unexpectedly, we found that the impact of ZIKV infection on trophoblast migration was due to the anti-viral response it generates, which is characterized by the expression of type I IFNβ and downstream ISGs. Indeed, treatment with IFNβ replicated ZIKV infection-induced inhibition of trophoblast attachment and migration.

Although mostly characterized for their ability to interfere with viral replication, IFNs, through specific ISGs, have immunomodulatory, cell differentiation, anti-angiogenic and pro-apoptotic effects (88). If left unchecked, the deleterious effects have been shown to produce complications such as autoimmune diseases, which have been associated with excessive or chronic type I IFN responses (3, 18, 19). Therefore, the regulation of type I IFN response is critical for an efficient immune response and maintenance of tissue homeostasis. We observed that the high levels of IFNβ expression in response to ZIKV infection had a detrimental effect on trophoblast function, consequently we sought to identify the mechanism associated with this effect.

Interestingly, the most predominant gene affected by viral infection was Twist1, a highly evolutionally conserved basic Helix-Loop-Helix (bHLH) transcriptional factor that functions as a master regulator of gastrulation and mesodermal development (89, 90);(91, 92). In addition to its role in embryogenesis, Twist1 has been found to be a key regulator in

the inflammatory processes by functioning as a regulator of the NFκB signaling pathway (93).Twist1, binds to E boxes present in the promoters of several NF-kB–dependent inflammatory cytokines, such as TNFα, IL-1 and IL-6, and suppresses cytokine production by blocking NF-κB–dependent transcriptional activation (39, 94). Sharif et al. reported the interaction between Type I interferons (IFNs), Twist1, and the NFκB pathway (40). They found that Type I IFNs suppressed the production of TNFα through the regulation of the expression of the receptor tyrosine kinase Axl and downstream induction of Twist1 (40); however, the type of interaction between Twist1 and type I IFN was not defined. Our findings reveled that as result of the Type I IFN response to ZIKV, IFNβ inhibits Twist1 expression, a necessary step to mount a strong anti-viral response; unfortunately, inhibition of Twist1 also will impact the capacity of the trophoblast to migrate and invade, two essential aspects for the success of the pregnancy.

In summary, we demonstrate that there is a direct interaction between Twist1 and IRF9, which leads to enhanced IRF9 transcriptional activity. These findings demonstrate a novel mechanism of antiviral awareness necessary for an early response.

Supplementary Material

Refer to Web version on PubMed Central for supplementary material.

Acknowledgments

We thank Ms. Alyssa Alday for her help with the preparation of the manuscript.

This work was supported in part by NIH grants NIAID 5R01AI145829-03, NICHD 1R01HD111146-01 and NIEHS 1P42ES030991-01A1 (GM).

References

1. Meizlish ML, Franklin RA, Zhou X, and Medzhitov R. 2021. Tissue Homeostasis and Inflammation. Annual Review of Immunology 39: 557–581.
2. Kulkarni OP, Lichtnekert J, Anders HJ, and Mulay SR. 2016. The Immune System in Tissue Environments Regaining Homeostasis after Injury: Is “Inflammation” Always Inflammation? Mediators Inflamm 2016: 2856213. [PubMed: 27597803]
3. Shaykhiev R, and Bals R. 2007. Interactions between epithelial cells and leukocytes in immunity and tissue homeostasis. J. Leuk. Biol 82: 1–15.
4. Janeway CA Jr. 2001. How the immune system protects the host from infection. Microbes Infect 3: 1167–1171. [PubMed: 11709297]
5. Iwasaki A, and Medzhitov R. 2010. Regulation of adaptive immunity by the innate immune system. Science 327: 291–295. [PubMed: 20075244]
6. Ivashkiv LB, and Donlin LT. 2014. Regulation of type I interferon responses. Nat Rev Immunol 14: 36–49. [PubMed: 24362405]
7. Dutia BM, Allen DJ, Dyson H, and Nash AA. 1999. Type I interferons and IRF-1 play a critical role in the control of a gammaherpesvirus infection. Virology 261: 173–179. [PubMed: 10497103]
8. Duncan CJA, Randall RE, and Hambleton S. 2021. Genetic Lesions of Type I Interferon Signalling in Human Antiviral Immunity. Trends Genet 37: 46–58. [PubMed: 32977999]
9. Trinchieri G 2010. Type I interferon: friend or foe? J Exp Med 207: 2053–2063. [PubMed: 20837696]

10. Ding J, Maxwell A, Adzibolosu N, Hu A, You Y, Liao A, and Mor G. 2022. Mechanisms of immune regulation by the placenta: Role of type I interferon and interferon-stimulated genes signaling during pregnancy*. Immunological Reviews 308: 9–24. [PubMed: 35306673]
11. Kell AM, and Gale M Jr. 2015. RIG-I in RNA virus recognition. Virology 479–480: 110–121.
12. Cavlar T, Ablasser A, and Hornung V. 2012. Induction of type I IFNs by intracellular DNA-sensing pathways. Immunol Cell Biol 90: 474–482. [PubMed: 22450802]
13. Stark GR, Cheon H, and Wang Y. 2018. Responses to Cytokines and Interferons that Depend upon JAKs and STATs. Cold Spring Harbor perspectives in biology 10.
14. Gough DJ, Messina NL, Clarke CJ, Johnstone RW, and Levy DE. 2012. Constitutive type I interferon modulates homeostatic balance through tonic signaling. Immunity 36: 166–174. [PubMed: 22365663]
15. Banninger G, and Reich NC. 2004. STAT2 Nuclear Trafficking*. Journal of Biological Chemistry 279: 39199–39206. [PubMed: 15175343]
16. Wong MT, and Chen SS. 2016. Emerging roles of interferon-stimulated genes in the innate immune response to hepatitis C virus infection. Cell Mol Immunol 13: 11–35. [PubMed: 25544499]
17. Levy DE, Kessler DS, Pine R, Reich N, and Darnell JE. 1988. Interferon-induced nuclear factors that bind a shared promoter element correlate with positive and negative transcriptional control. Genes & Development 2: 383–393. [PubMed: 3371658]
18. Schoggins JW, Wilson SJ, Panis M, Murphy MY, Jones CT, Bieniasz P, and Rice CM. 2011. A diverse range of gene products are effectors of the type I interferon antiviral response. Nature 472: 481–485. [PubMed: 21478870]
19. Pestka S, Krause CD, and Walter MR. 2004. Interferons, interferon-like cytokines, and their receptors. Immunol Rev 202: 8–32. [PubMed: 15546383]
20. Taniguchi T, and Takaoka A. 2001. A weak signal for strong responses: interferon-alpha/beta revisited. Nature Reviews Molecular Cell Biology 2: 378–386. [PubMed: 11331912]
21. Mor G, Aldo P, and Alvero AB. 2017. The unique immunological and microbial aspects of pregnancy. Nat Rev Immunol 17: 469–482. [PubMed: 28627518]
22. Costello MJ, Joyce SK, and Abrahams VM. 2007. NOD protein expression and function in first trimester trophoblast cells. Am J Reprod Immunol 57: 67–80. [PubMed: 17156193]
23. Abrahams VM, Aldo PB, Murphy SP, Visintin I, Koga K, Wilson G, Romero R, Sharma S, and Mor G. 2008. TLR6 modulates first trimester trophoblast responses to peptidoglycan. J Immunol 180: 6035–6043. [PubMed: 18424724]
24. Abrahams VM, Bole-Aldo P, Kim YM, Straszewski-Chavez SL, Chaiworapongsa T, Romero R, and Mor G. 2004. Divergent trophoblast responses to bacterial products mediated by TLRs. J Immunol 173: 4286–4296. [PubMed: 15383557]
25. Abrahams VM, Fahey JV, Schaefer TM, Wright JA, Wira CR, and Mor G. 2005. Stimulation of first trimester trophoblast cells with Poly(I:C) induces SLPI secretion. AJRI 53: 280 ASRI205–204.
26. Abrahams VM, Kim YM, Straszewski SL, Romero R, and Mor G. 2004. Macrophages and apoptotic cell clearance during pregnancy. Am J Reprod Immunol 51: 275–282. [PubMed: 15212680]
27. Abrahams VM, Romero R, and Mor G. 2005. TLR-3 and TLR-4 mediate differential chemokine production and immune cell recruitment by first trimester trophoblast cells. AJRI 53: 279.
28. Racicot K, Kwon JY, Aldo P, Abrahams V, El-Guindy A, Romero R, and Mor G. 2016. Type I Interferon Regulates the Placental Inflammatory Response to Bacteria and is Targeted by Virus: Mechanism of Polymicrobial Infection-Induced Preterm Birth. Am J Reprod Immunol 75: 451–460. [PubMed: 26892235]
29. Kwon JY, Aldo P, You Y, Ding J, Racicot K, Dong X, Murphy J, Glukshtad G, Silasi M, Peng J, Wen L, Abrahams VM, Romero R, and Mor G. 2018. Relevance of placental type I interferon beta regulation for pregnancy success. Cell Mol Immunol.
30. Silasi M, Cardenas I, Kwon JY, Racicot K, Aldo P, and Mor G. 2015. Viral infections during pregnancy. Am J Reprod Immunol 73: 199–213. [PubMed: 25582523]

31. Kwon JY, Aldo P, You Y, Ding J, Racicot K, Dong X, Murphy J, Glukshtad G, Silasi M, Peng J, Wen L, Abrahams VM, Romero R, and Mor G. 2018. Relevance of placental type I interferon beta regulation for pregnancy success. Cell Mol Immunol 15: 1010–1026. [PubMed: 29907882]
32. Yockey LJ, Jurado KA, Arora N, Millet A, Rakib T, Milano KM, Hastings AK, Fikrig E, Kong Y, Horvath TL, Weatherbee S, Kliman HJ, Coyne CB, and Iwasaki A. 2018. Type I interferons instigate fetal demise after Zika virus infection. Science immunology 3.
33. Dudley DM, Van Rompay KK, Coffey LL, Ardeshir A, Keesler RI, Bliss-Moreau E, Grigsby PL, Steinbach RJ, Hirsch AJ, MacAllister RP, Pecoraro HL, Colgin LM, Hodge T, Streblow DN, Tardif S, Patterson JL, Tamhankar M, Seferovic M, Aagaard KM, Martín CS, Chiu CY, Panganiban AT, Veazey RS, Wang X, Maness NJ, Gilbert MH, Bohm RP, Adams Waldorf KM, Gale M Jr., Rajagopal L, Hotchkiss CE, Mohr EL, Capuano SV 3rd, Simmons HA, Mejia A, Friedrich TC, Golos TG, and O'Connor DH. 2018. Miscarriage and stillbirth following maternal Zika virus infection in nonhuman primates. Nat Med 24: 1104–1107. [PubMed: 29967348]
34. van der Eijk AA, van Genderen PJ, Verdijk RM, Reusken CB, Mögling R, van Kampen JJA, Widagdo W, Aron GI, GeurtsvanKessel CH, Pas SD, Raj VS, Haagmans BL, and Koopmans MPG. 2016. Miscarriage Associated with Zika Virus Infection. New England Journal of Medicine 375: 1002–1004. [PubMed: 27463941]
35. Schaub B, Monthieux A, Najioullah F, Harte C, Césaire R, Jolivet E, and Voluménie J-L. 2016. Late miscarriage: another Zika concern? European Journal of Obstetrics & Gynecology and Reproductive Biology 207: 240–241. [PubMed: 27837933]
36. Quicke KM, Bowen JR, Johnson EL, McDonald CE, Ma H, O'Neal JT, Rajakumar A, Wrammert J, Rimawi BH, Pulendran B, Schinazi RF, Chakraborty R, and Suthar MS. 2016. Zika Virus Infects Human Placental Macrophages. Cell host & microbe 20: 83–90. [PubMed: 27247001]
37. Lee YB, Bantounas I, Lee DY, Phylactou L, Caldwell MA, and Uney JB. 2009. Twist-1 regulates the miR-199a/214 cluster during development. Nucleic Acids Res 37: 123–128. [PubMed: 19029138]
38. Ahn JH, Park HR, Park CW, Park DW, and Kwak-Kim J. 2017. Expression of TWIST in the first-trimester trophoblast and decidual tissue of women with recurrent pregnancy losses. Am J Reprod Immunol 78.
39. Zheng S, Hedl M, and Abraham C. 2015. Twist1 and Twist2 Contribute to Cytokine Downregulation following Chronic NOD2 Stimulation of Human Macrophages through the Coordinated Regulation of Transcriptional Repressors and Activators. J Immunol 195: 217–226. [PubMed: 26019273]
40. Sharif MN, Sosic D, Rothlin CV, Kelly E, Lemke G, Olson EN, and Ivashkiv LB. 2006. Twist mediates suppression of inflammation by type I IFNs and Axl. J Exp Med 203: 1891–1901. [PubMed: 16831897]
41. Ding J, Aldo P, Roberts CM, Stabach P, Liu H, You Y, Qiu X, Jeong J, Maxwell A, Lindenbach B, Braddock D, Liao A, and Mor G. 2021. Placenta-derived interferon-stimulated gene 20 controls ZIKA virus infection. EMBO Rep: e52450. [PubMed: 34405956]
42. Potter JA, Tong M, Aldo P, Kwon JY, Pitruzzello M, Mor G, and Abrahams VM. 2020. Viral infection dampens human fetal membrane type I interferon responses triggered by bacterial LPS. J Reprod Immunol 140: 103126. [PubMed: 32289593]
43. You Y, Stelzl P, Zhang Y, Porter J, Liu H, Liao AH, Aldo PB, and Mor G. 2019. Novel 3D in vitro models to evaluate trophoblast migration and invasion. Am J Reprod Immunol 81: e13076. [PubMed: 30582662]
44. Alexandrova M, Manchorova D, You Y, Mor G, Dimitrova V, and Dimova T. 2022. Functional HLA-C expressing trophoblast spheroids as a model to study placental-maternal immune interactions during human implantation. Scientific reports 12: 10224. [PubMed: 35715452]
45. Alexandrova M, Manchorova D, You Y, Mor G, Dimitrova V, and Dimova T. 2022. Functional HLA-C expressing trophoblast spheroids as a model to study placental–maternal immune interactions during human implantation. Scientific reports 12: 10224. [PubMed: 35715452]
46. Sanjana NE, Shalem O, and Zhang F. 2014. Improved vectors and genome-wide libraries for CRISPR screening. Nature methods 11: 783–784. [PubMed: 25075903]

47. Walter DM, Venancio OS, Buza EL, Tobias JW, Deshpande C, Gudiel AA, Kim-Kiselak C, Cicchini M, Yates TJ, and Feldser DM. 2017. Systematic In Vivo Inactivation of Chromatin-Regulating Enzymes Identifies Setd2 as a Potent Tumor Suppressor in Lung Adenocarcinoma. Cancer Research 77: 1719–1729. [PubMed: 28202515]
48. Stewart SA, Dykxhoorn DM, Palliser D, Mizuno H, Yu EY, An DS, Sabatini DM, Chen IS, Hahn WC, Sharp PA, Weinberg RA, and Novina CD. 2003. Lentivirus-delivered stable gene silencing by RNAi in primary cells. RNA 9: 493–501. [PubMed: 12649500]
49. Straszewski-Chavez SL, Abrahams VM, Alvero AB, Aldo PB, Ma Y, Guller S, Romero R, and Mor G. 2009. The isolation and characterization of a novel telomerase immortalized first trimester trophoblast cell line, Swan 71. Placenta 30: 939–948. [PubMed: 19766308]
50. Jeong DS, Kim MH, and Lee JY. 2021. Depletion of CTCF disrupts PSG gene expression in the human trophoblast cell line Swan 71. FEBS Open Bio 11: 804–812.
51. Liu H, Wang L, Wang Y, Zhu Q, Aldo P, Ding J, Mor G, and Liao A. 2020. Establishment and characterization of a new human first trimester Trophoblast cell line, AL07. Placenta 100: 122–132. [PubMed: 32927240]
52. Visintin I, Feng Z, Longton G, Ward DC, Alvero AB, Lai Y, Tenthorey J, Leiser A, Flores-Saaib R, Yu H, Azori M, Rutherford T, Schwartz PE, and Mor G. 2008. Diagnostic markers for early detection of ovarian cancer. Clin Cancer Res 14: 1065–1072. [PubMed: 18258665]
53. Phipson B, Lee S, Majewski IJ, Alexander WS, and Smyth GK. 2016. Robust Hyperparameter Estimation Protects against Hypervariable Genes and Improves Power to Detect Differential Expression. Ann Appl Stat 10: 946–963. [PubMed: 28367255]
54. Ritchie ME, Phipson B, Wu D, Hu Y, Law CW, Shi W, and Smyth GK. 2015. limma powers differential expression analyses for RNA-sequencing and microarray studies. Nucleic Acids Res 43: e47. [PubMed: 25605792]
55. Ahsan S, and Draghici S. 2017. Identifying Significantly Impacted Pathways and Putative Mechanisms with iPathwayGuide. Curr Protoc Bioinformatics 57: 7 15 11–17 15 30.
56. Donato M, Xu Z, Tomoiaga A, Granneman JG, Mackenzie RG, Bao R, Than NG, Westfall PH, Romero R, and Draghici S. 2013. Analysis and correction of crosstalk effects in pathway analysis. Genome Res 23: 1885–1893. [PubMed: 23934932]
57. Draghici S, Khatri P, Tarca AL, Amin K, Done A, Voichita C, Georgescu C, and Romero R. 2007. A systems biology approach for pathway level analysis. Genome Res 17: 1537–1545. [PubMed: 17785539]
58. Tarca AL, Draghici S, Khatri P, Hassan SS, Mittal P, Kim JS, Kim CJ, Kusanovic JP, and Romero R. 2009. A novel signaling pathway impact analysis. Bioinformatics 25: 75–82. [PubMed: 18990722]
59. Marini F, and Binder H. 2019. pcaExplorer: an R/Bioconductor package for interacting with RNA-seq principal components. BMC Bioinformatics 20: 331. [PubMed: 31195976]
60. Gu Z, Eils R, and Schlesner M. 2016. Complex heatmaps reveal patterns and correlations in multidimensional genomic data. Bioinformatics 32: 2847–2849. [PubMed: 27207943]
61. Wickham H 2016. ggplot2: Elegant Graphics for Data Analysis. Springer-Verlag New York.
62. Edwards RG 1988. Human uterine endocrinology and the implantation window. Ann N Y Acad Sci 541: 445–454. [PubMed: 3195928]
63. Edwards RG 1995. Physiological and molecular aspects of human implantation. Hum Reprod 10 Suppl 2: 1–13.
64. Cross JC, Hemberger M, Lu Y, Nozaki T, Whiteley K, Masutani M, and Adamson SL. 2002. Trophoblast functions, angiogenesis and remodeling of the maternal vasculature in the placenta. Mol Cell Endocrinol 187: 207–212. [PubMed: 11988329]
65. Adamson SL, Lu Y, Whiteley KJ, Holmyard D, Hemberger M, Pfarrer C, and Cross JC. 2002. Interactions between trophoblast cells and the maternal and fetal circulation in the mouse placenta. Dev Biol 250: 358–373. [PubMed: 12376109]
66. Aldo PB, Mulla MJ, Romero R, Mor G, and Abrahams VM. 2010. Viral ssRNA induces first trimester trophoblast apoptosis through an inflammatory mechanism. Am J Reprod Immunol 64: 27–37. [PubMed: 20175771]

67. Kovats S, Main E, and Librach C. 1990. HLA-G expressed in human trophoblast. Science 248: 220–223. [PubMed: 2326636]
68. Tilburgs T 2021. Chapter 2 - Presentation and recognition of placental, fetal, and pathogen-derived antigens in human pregnancy. In Reproductive Immunology. Mor G, ed. Academic Press. 23–37.
69. Kraus TA, Lau JF, Parisien J-P, and Horvath CM. 2003. A Hybrid IRF9-STAT2 Protein Recapitulates Interferon-stimulated Gene Expression and Antiviral Response*. Journal of Biological Chemistry 278: 13033–13038. [PubMed: 12574168]
70. Paul A, Tang TH, and Ng SK. 2018. Interferon Regulatory Factor 9 Structure and Regulation. Frontiers in immunology 9: 1831. [PubMed: 30147694]
71. Suprunenko T, and Hofer MJ. 2016. The emerging role of interferon regulatory factor 9 in the antiviral host response and beyond. Cytokine Growth Factor Rev 29: 35–43. [PubMed: 26987614]
72. Luker KE, Pica CM, Schreiber RD, and Piwnica-Worms D. 2001. Overexpression of IRF9 confers resistance to antimicrotubule agents in breast cancer cells. Cancer Res 61: 6540–6547. [PubMed: 11522652]
73. Jiang DS, Luo YX, Zhang R, Zhang XD, Chen HZ, Zhang Y, Chen K, Zhang SM, Fan GC, Liu PP, Liu DP, and Li H. 2014. Interferon regulatory factor 9 protects against cardiac hypertrophy by targeting myocardin. Hypertension 63: 119–127. [PubMed: 24144649]
74. Rauch I, Rosebrock F, Hainzl E, Heider S, Majoros A, Wienerroither S, Strobl B, Stockinger S, Kenner L, Müller M, and Decker T. 2015. Noncanonical Effects of IRF9 in Intestinal Inflammation: More than Type I and Type III Interferons. Mol Cell Biol 35: 2332–2343. [PubMed: 25918247]
75. Huber M, Suprunenko T, Ashhurst T, Marbach F, Raifer H, Wolff S, Strecker T, Viengkhou B, Jung SR, Obermann HL, Bauer S, Xu HC, Lang PA, Tom A, Lang KS, King NJC, Campbell IL, and Hofer MJ. 2017. IRF9 Prevents CD8(+) T Cell Exhaustion in an Extrinsic Manner during Acute Lymphocytic Choriomeningitis Virus Infection. J Virol 91.
76. Paun A, and Pitha PM. 2007. The IRF family, revisited. Biochimie 89: 744–753. [PubMed: 17399883]
77. Kessler DS, Veals SA, Fu XY, and Levy DE. 1990. Interferon-alpha regulates nuclear translocation and DNA-binding affinity of ISGF3, a multimeric transcriptional activator. Genes Dev 4: 1753–1765. [PubMed: 2249773]
78. Maxwell AJ, You Y, Aldo PB, Zhang Y, Ding J, and Mor G. 2021. Chapter 1 - The role of the immune system during pregnancy: General concepts. In Reproductive Immunology. Mor G, ed. Academic Press. 1–21.
79. Marr Nico, Wang Ting-I, Kam SHY, Shen Hu, Sharma AA, Angie Lam, Markowski Joy, Solimano Alfonso, Lavoie PM, and Turvey SE. 2014. Attenuation of Respiratory Syncytial Virus–Induced and RIG-I–Dependent Type I IFN Responses in Human Neonates and Very Young Children. The Journal of Immunology 192: 948–957. [PubMed: 24391215]
80. Shi L, Tu N, and Patterson PH. 2005. Maternal influenza infection is likely to alter fetal brain development indirectly: the virus is not detected in the fetus. Int J Dev Neurosci 23: 299–305. [PubMed: 15749254]
81. Romero R, Espinoza J, Goncalves LF, Kusanovic JP, Friel L, and Hassan S. 2007. The role of inflammation and infection in preterm birth. Semin Reprod Med 25: 21–39. [PubMed: 17205421]
82. Romero R, Xu Y, Plazyo O, Chaemsaithong P, Chaiworapongsa T, Unkel R, Than NG, Chiang PJ, Dong Z, Xu Z, Tarca AL, Abrahams VM, Hassan SS, Yeo L, and Gomez-Lopez N. 2016. A Role for the Inflammasome in Spontaneous Labor at Term. Am J Reprod Immunol.
83. Dudley DM, Van Rompay KK, Coffey LL, Ardeshir A, Keesler RI, Bliss-Moreau E, Grigsby PL, Steinbach RJ, Hirsch AJ, MacAllister RP, Pecoraro HL, Colgin LM, Hodge T, Streblow DN, Tardif S, Patterson JL, Tamhankar M, Seferovic M, Aagaard KM, Martín CS-S, Chiu CY, Panganiban AT, Veazey RS, Wang X, Maness NJ, Gilbert MH, Bohm RP, Adams Waldorf KM, Gale M, Rajagopal L, Hotchkiss CE, Mohr EL, Capuano SV, Simmons HA, Mejia A, Friedrich TC, Golos TG, and O'Connor DH. 2018. Miscarriage and stillbirth following maternal Zika virus infection in nonhuman primates. Nature Med. 24: 1104–1107. [PubMed: 29967348]

84. Thirkill TL, Lowe K, Vedagiri H, Blankenship TN, Barakat AI, and Douglas GC. 2005. Macaque trophoblast migration is regulated by RANTES. Experimental Cell Research 305: 355–364. [PubMed: 15817160]

85. You Y, Stelzl P, Joseph DN, Aldo PB, Maxwell AJ, Dekel N, Liao A, Whirledge S, and Mor G. 2021. TNF-α Regulated Endometrial Stroma Secretome Promotes Trophoblast Invasion. Frontiers in immunology 12: 737401. [PubMed: 34790194]

86. George JS, Mortimer R, and Anchan RM. 2022. Chapter 15 - The role of reproductive immunology in recurrent pregnancy loss and repeated implantation failure. In Immunology of Recurrent Pregnancy Loss and Implantation Failure. Kwak-Kim J, ed. Academic Press. 223–240.

87. Hoen B, Schaub B, Funk AL, Ardillon V, Boullard M, Cabié A, Callier C, Carles G, Cassadou S, Césaire R, Douine M, Herrmann-Storck C, Kadhel P, Laouénan C, Madec Y, Monthieux A, Nacher M, Najioullah F, Rousset D, Ryan C, Schepers K, Stegmann-Planchard S, Tressières B, Voluménie J-L, Yassinguezo S, Janky E, and Fontanet A. 2018. Pregnancy Outcomes after ZIKV Infection in French Territories in the Americas. New England Journal of Medicine 378: 985–994. [PubMed: 29539287]

88. Garcia-Sastre A, and Biron CA. 2006. Type 1 interferons and the virus-host relationship: a lesson in detente. Science 312: 879–882. [PubMed: 16690858]

89. Thisse B, Stoetzel C, Gorostiza-Thisse C, and Perrin-Schmitt F. 1988. Sequence of the twist gene and nuclear localization of its protein in endomesodermal cells of early Drosophila embryos. The EMBO Journal 7: 2175–2183. [PubMed: 3416836]

90. Thisse B, el Messal M, and Perrin-Schmitt F. 1987. The twist gene: isolation of a Drosophila zygotic gene necessary for the establishment of dorsoventral pattern. Nucleic Acids Res 15: 3439–3453. [PubMed: 3106932]

91. Bialek P, Kern B, Yang X, Schrock M, Sosic D, Hong N, Wu H, Yu K, Ornitz DM, Olson EN, Justice MJ, and Karsenty G. 2004. A twist code determines the onset of osteoblast differentiation. Dev Cell 6: 423–435. [PubMed: 15030764]

92. Cheng GZ, Zhang W, and Wang LH. 2008. Regulation of cancer cell survival, migration, and invasion by Twist: AKT2 comes to interplay. Cancer Research 68: 957–960. [PubMed: 18281467]

93. Li S, Kendall SE, Raices R, Finlay J, Covarrubias M, Liu Z, Lowe G, Lin YH, Teh YH, Leigh V, Dhillon S, Flanagan S, Aboody KS, and Glackin CA. 2012. TWIST1 associates with NF-kappaB subunit RELA via carboxyl-terminal WR domain to promote cell autonomous invasion through IL8 production. BMC biology 10: 73. [PubMed: 22891766]

94. Roberts CM, Tran MA, Pitruzzello MC, Wen W, Loeza J, Dellinger TH, Mor G, and Glackin CA. 2016. TWIST1 drives cisplatin resistance and cell survival in an ovarian cancer model, via upregulation of GAS6, L1CAM, and Akt signalling. Scientific reports 6: 37652. [PubMed: 27876874]

- ZIKV infection inhibits Twsit1 expression and trophoblast migration.
- Twist1 interacts with IRF9 and provides protection against ZIKV infection.
- Interferon beta inhibits Twist1 expression.

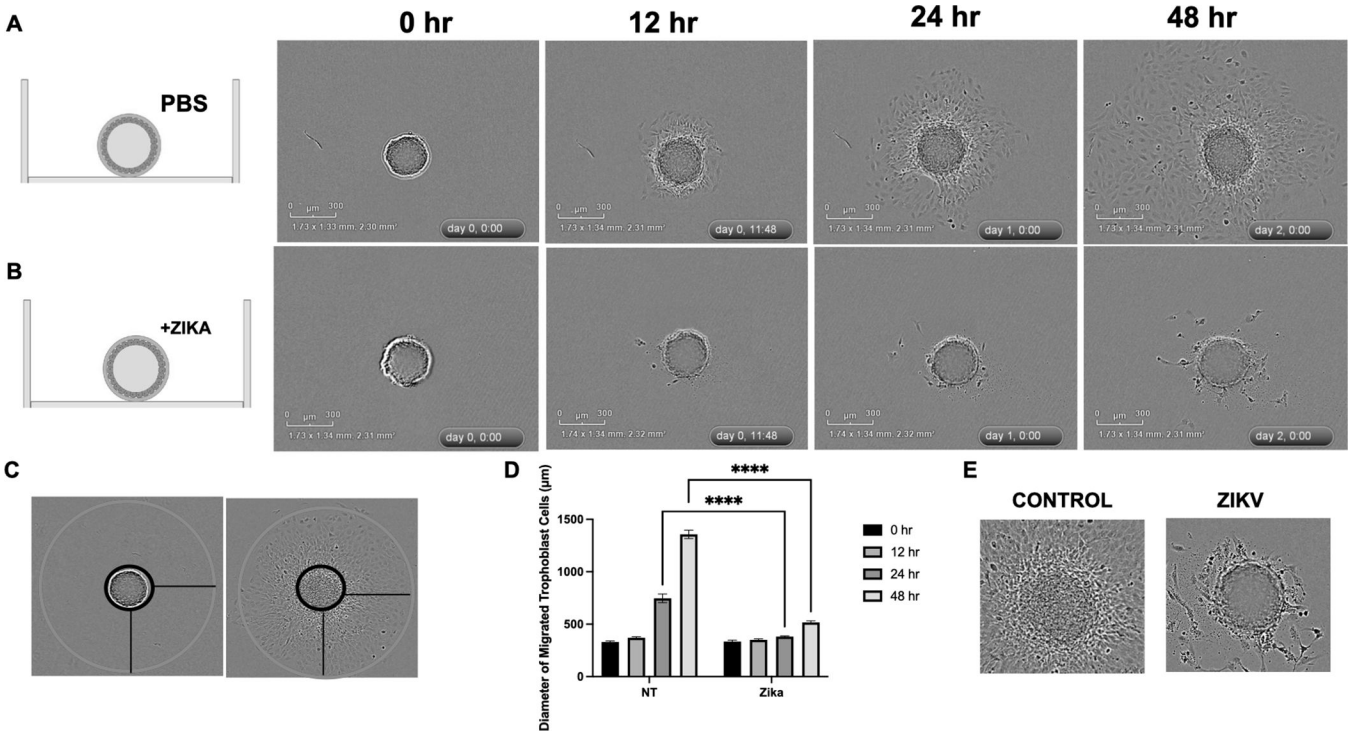

Figure 1. ZIKV infection inhibits trophoblast migration.

Blastocyst-like structures (BLS) were established from Sw71 human first trimester trophoblast cells as described in Materials and Methods Section and exposed to ZIKV or vehicle control for up to 48h. Trophoblast migration was monitored using live imaging.

A. Time dependent migration of BLS treated with Vehicle. Note attachment to the plate and migration of trophoblast cells from BLS.

B. Migration of BLS treated with ZIKV. Note that BLS exposed to ZIKV are able to attach but not migrate. Representative images from 10 independent experiments each in triplicate.

C. Method of quantification of trophoblast migration. Black circle is drawn corresponding to the outline of attached BLS. Red circle corresponds to outline of migrating cells at the latest time-point. Distance between the black and red circles are quantified (um) and used as measure of migration.

D. Quantification of trophoblast migration. Data are presented as mean ±SEM. n=10 independent experiments, each one in triplicate. ****= p=0.0001.

E. Representative images of BLS migration comparing Vehicle-treated and ZIKV-infected BSL.

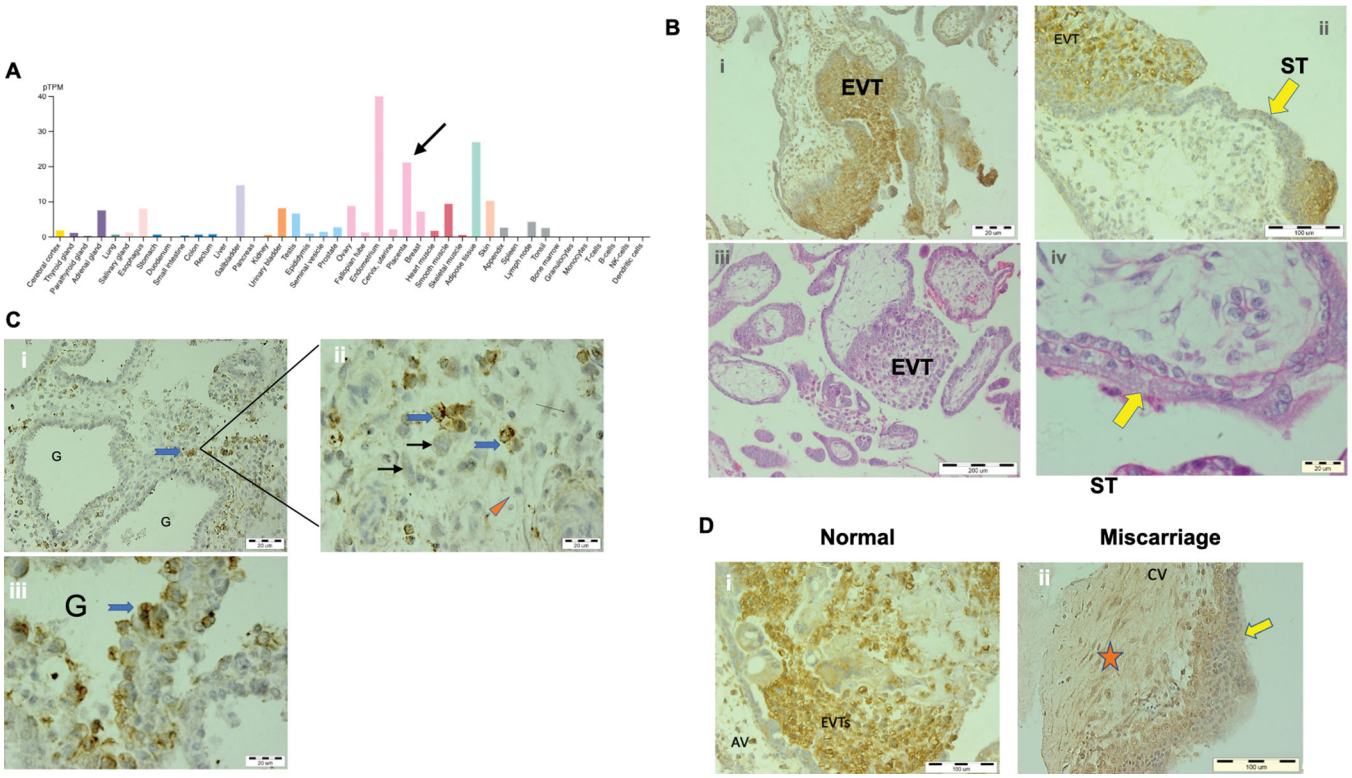

Figure 2. Twist Expression in the human placenta.

A. Expression of Twist1 in human tissues (obtained from Human Protein ATLAS). Note highly expression in reproductive tissues such as ovary, endometrium, breast and placenta.

B. IHC for Twist1 in first trimester human placentas: i, anchoring region EVT and ii, placental villi showed positive reactivity for Twist1. Cytotrophoblast and syncytiotrophoblast were negative; iii, H&E of anchoring region; iv, H&E of villi. Representative images of n=12 first trimester placentas.

C. Blue arrows point to Twist1 positive EVT cells in decidua (i-ii) and spiral arteries (iii); Immune cells are Twist1 negative (red arrow). Representative images of n=12 first trimester placentas.

D. Differential expression of Twist1 in placental samples obtained from elective termination (i) and miscarriage (ii). Note the decrease Twist expression in miscarriage samples. Representative images of 12 normal placentas and 6 miscarriages.

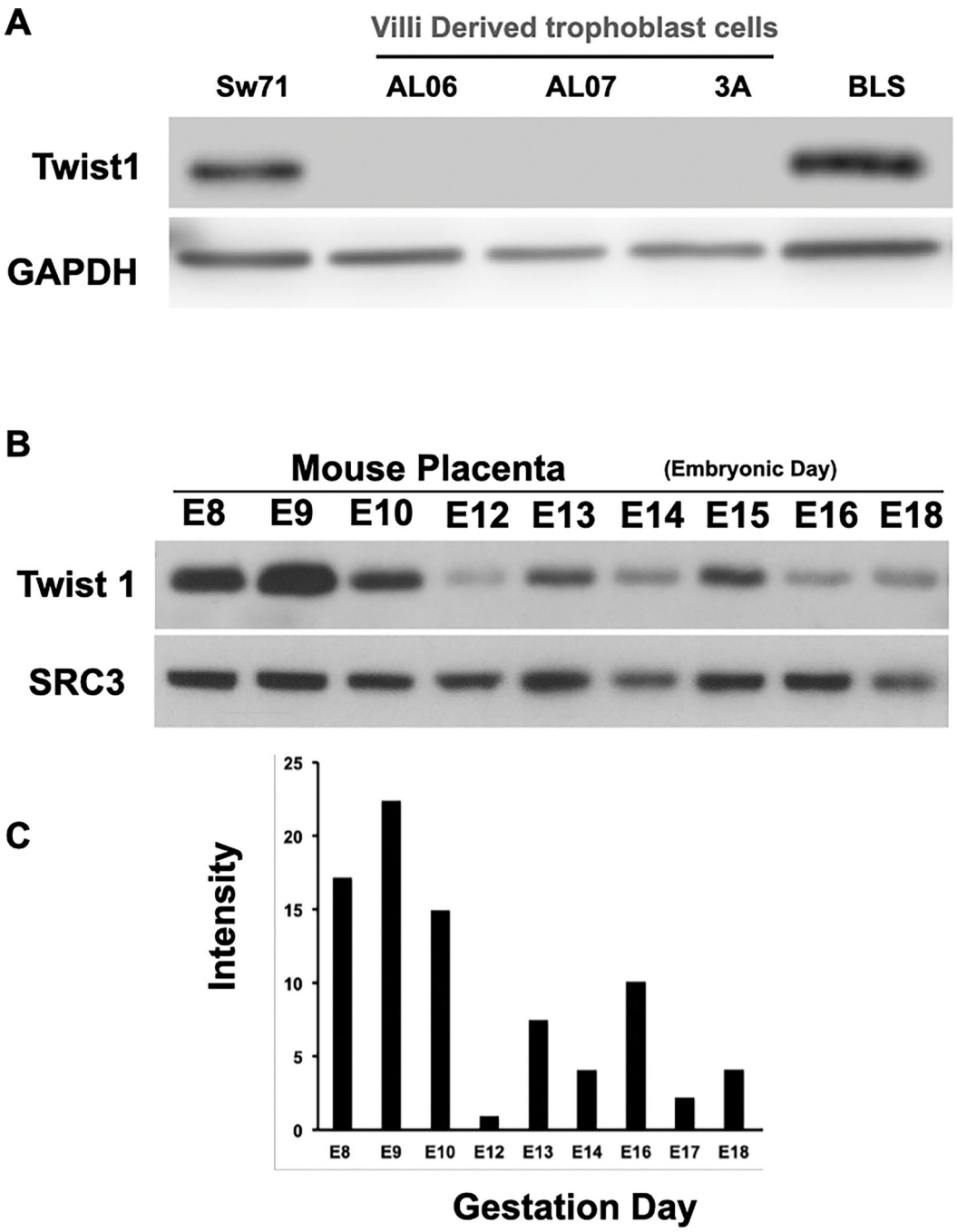

Figure 3. Twist1 expression in first trimester trophoblast cell lines.

A. Western blot analysis for Twist1 in cell lines Sw71, ALO6, ALO7 and 3A and in BLS. Note Twist1 positive expression only in Sw71 and BLS, which have migratory capacity. Representative figures of three independent experiments.

B. Temporal expression of Twist1 in mouse placenta. Placental samples were collected during from pregnant mice from E8-E18. Representative experiment of 15–18 placentas per time obtained from 3 individual pregnant mice for each day.

C. Quantification of Twist1 expression in placental samples throughout pregnancy. Note the high levels of Twist1 protein expression during early placentation (E-8-E10). 15–18 placentas per time obtained from 3 individual pregnant mice for each day.

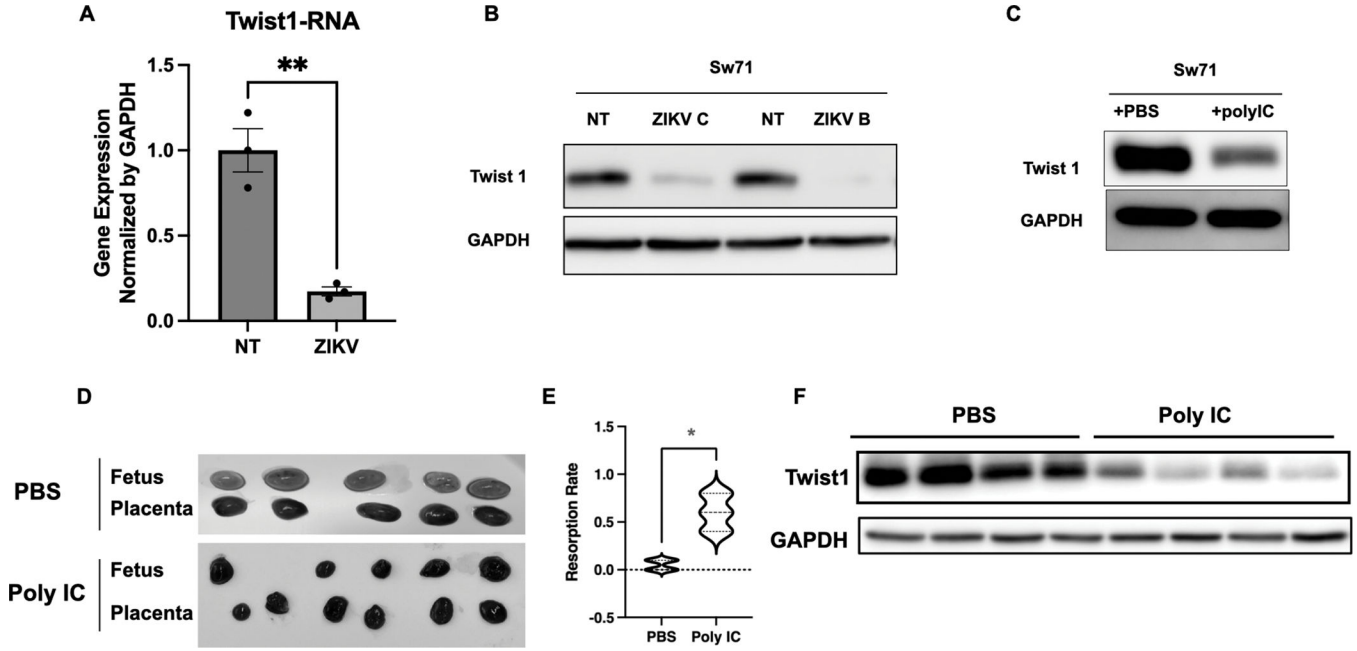

Figure 4. Effect of ZIKV infection on Twist1 expression in trophoblast cells

A. Sw71 first trimester trophoblast cell line was infected with ZIKV for 1 h and Twist1 mRNA was quantified by qPCR. Note significant decrease in Twist1 mRNA expression during ZIKV infection. N=6 independent experiments in triplicate. **=p=0.001

B. Sw71 first trimester trophoblast cell line was infected with ZIKV for 1 h and Twist1 protein levels were detected by Western blot. N=6 independent experiments in triplicate. ZIKV C = Zika Cambodia; ZIKV B = Zika Brazil

C. Sw71 first trimester trophoblast cell line was treated with PolyIc or PBS Control and Twist1 protein levels were detected by Western blot. N=6 independent experiments in triplicate.

D. Pregnant mice were injected with Poly IC on day E14.5 and placental and fetal morphology evaluated 24h later. Note placental and fetal in the treated group. Representative of 24 placental samples. n=4 mice per group

E. Quantification of fetal resorption form experiment in D.

F. Western blot analysis for Twist1 expression in placental samples from mice treated with Poly I C. Note the decrease in Twist1 protein expression in placental samples from Poly I C treated mice. Mice were injected on day E14.5 and samples were collected 4 h post injection. N=5 pregnant mice per group. Each mouse had an average of 6–8 placentas.

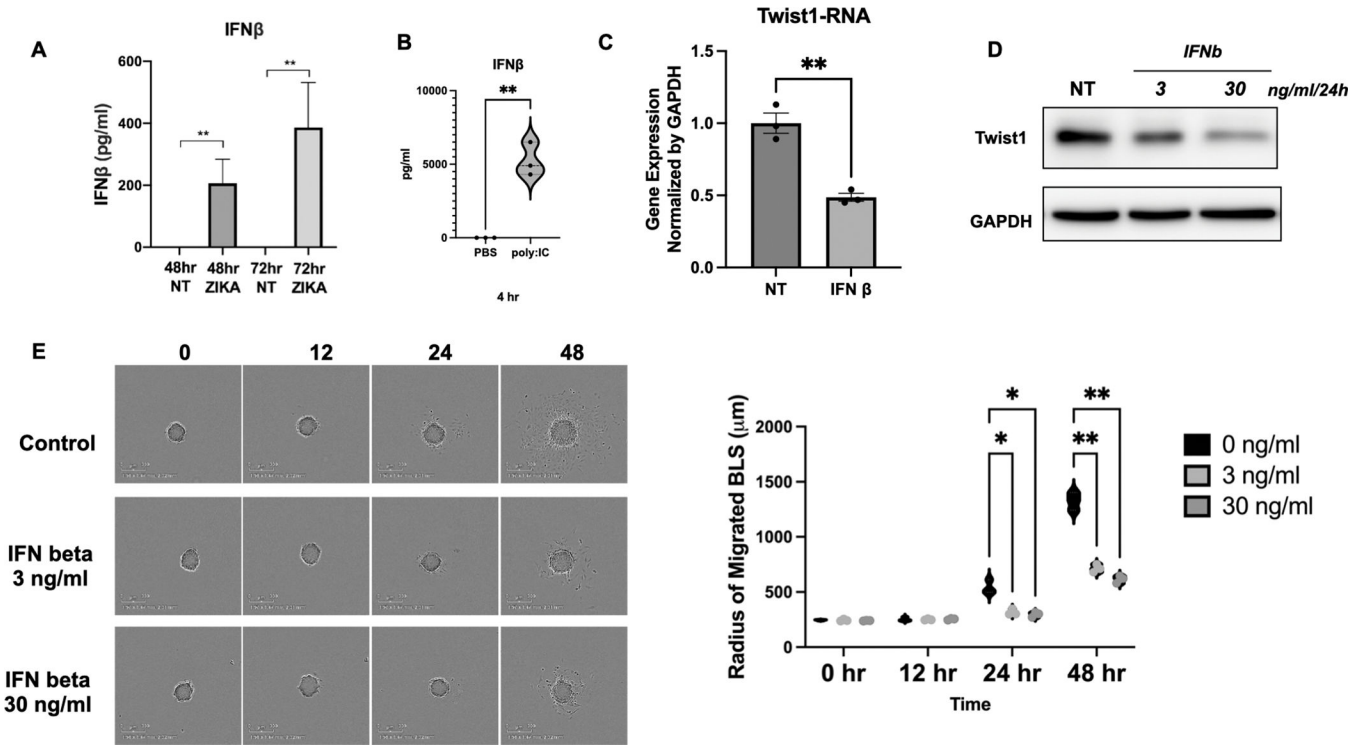

Figure 5. IFNβ induced by ZIKV infection inhibits Twit1 expression.

A. Sw71 first trimester trophoblast cell line was infected with ZIKV for 48h and 72h and IFN**β** was quantified by ELISA. N=6 independent experiments in triplicate. **=p>0.001

B. Sw71 first trimester trophoblast cell line was treated with **Poly IC** and IFN**β** was quantified by ELISA. N=6 independent experiments in triplicate **=p=0.0001

C. Sw71 first trimester trophoblast cell line was treated with IFNβ and Twist1 expression was measured by qPCR. **=p=0.0001. n=3 independent experiments in triplicates.

D. Sw71 first trimester trophoblast cell line was treated with IFNβ and Twist1 expression was measured by Western blot. Note the decrease on Twist expression following 24h treatment with IFNβ. N=3 independent experiments in triplicate

E. BLS were incubated in the presence of IFNβ (3 or 30 ng/ml) for 48h. Trophoblast migration was monitored by live imaging. Representative image of n=6 independent experiments in triplicate.

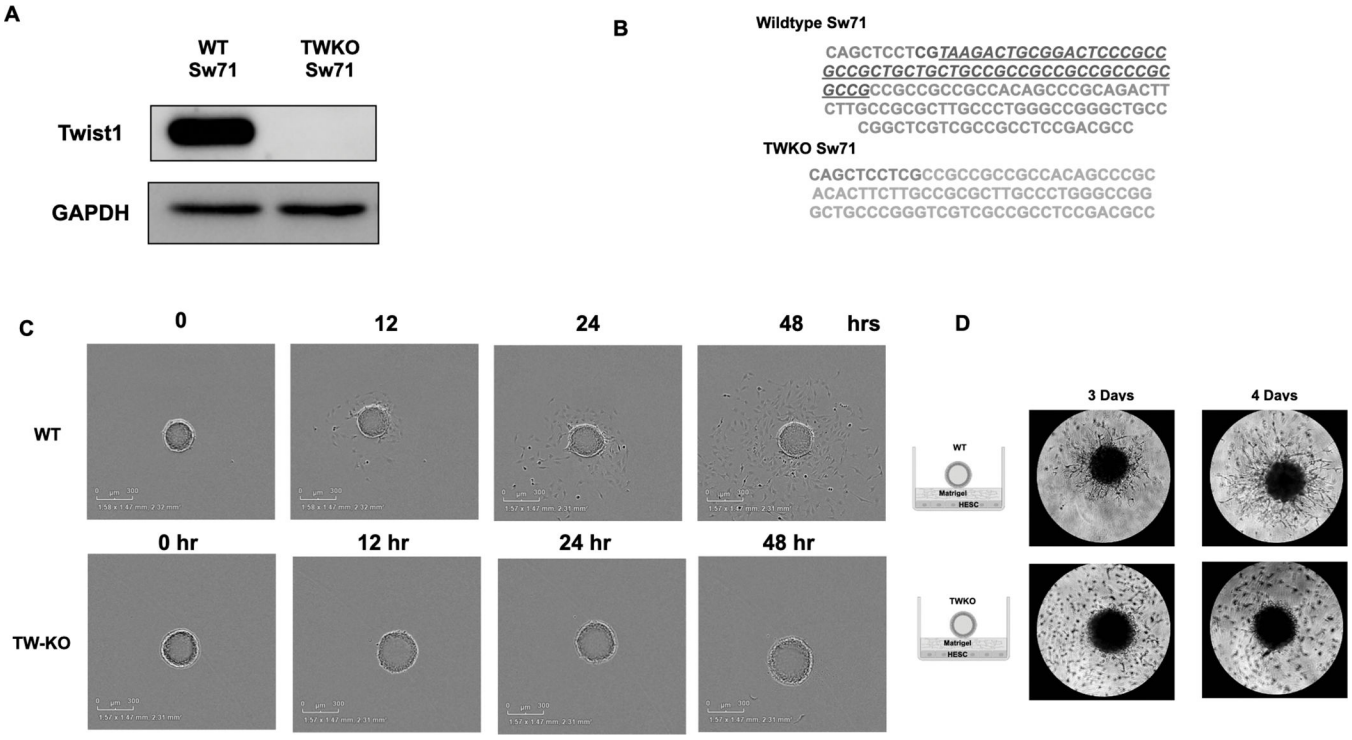

Figure 6. Characterization of a Twist1-deficient Sw71 trophoblast cell line

A. Twist1 was knocked out in Sw.71 first-trimester trophoblast cell line using CRISPR/Cas9 as described in the methods section. Western blot analysis for Twist1 expression in wild type Sw71 trophoblast cells and Twist deficient clone (TWKO) showed a successful Twist1 KO.

B. Sequencing results showing wild type Twist1 and deletion of Twist1 in TWKO cells. Sequence targeted by guide RNA sequence is shown red. Deleted sequence is shown in blue.

C. Migration assay comparing BLS formed with Sw.71 wild type and BLS formed with Sw.71 TWKO cells. Representative image of n=10 independent experiments in triplicate

D. In vitro model of trophoblast invasion. BLS were transferred to wells containing stromal cells layered with Matrigel. WT Sw71 trophoblast cells develop projections within the Matrigel, a sign of trophoblast invasion. No invasion was observed in BLS formed with Sw71 TWKO cells. Representative image of 10 independent experiments in triplicates

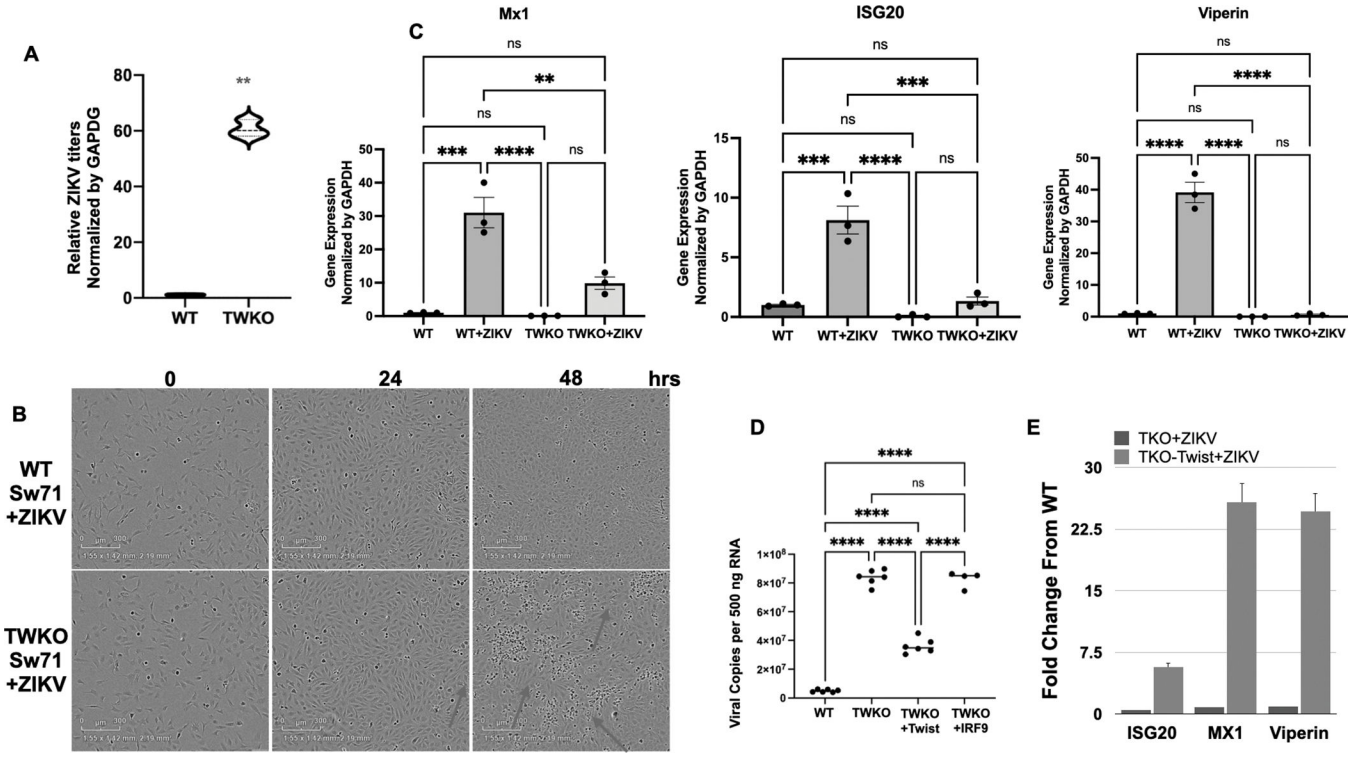

Figure 7. Sw71 TWKO cells are susceptible to ZIKV infection.

A. Wild type (WT) and Twist-KO Sw71 trophoblast cells (TWKO) were infected with ZIKV. Viral titers were determined by qPCR. Note the significant difference in viral titers between WT and Twist-KO. N=6 independent experiments done in triplicate. **=p>0.002

B. Twist-KO Sw71 trophoblast cells (TWKO) undergo cell death following ZIKV infection. No cell death was observed in WT cells. Representative images of 6 independent experiments done in triplicate.

C. Wild type (WT) and Twist-KO Sw71 trophoblast cells (TWKO) were infected with ZIKV and expression anti-viral ISGs (Mx1, ISG20 and Viperin) were determined by qPCR. N=3 independent experiments in triplicate **=p>0.001; ***=p.005; ****=p>0.0001

D. Twist1 or IRF9 were overexpressed in Twist-KO Sw71 trophoblast cells (TWKO). Cultures were then infected with ZIKV and viral titers were quantified. Overexpression of Twist1 but not IRF9 restored antiviral response. N=6 independent experiments in triplicate

E. Twsit1 transcomplementation in Sw71-KO cells reinstate the expression of ISGs in response to ZIKV infection. N=3 independent experiments in triplicate ****=p>0.0001

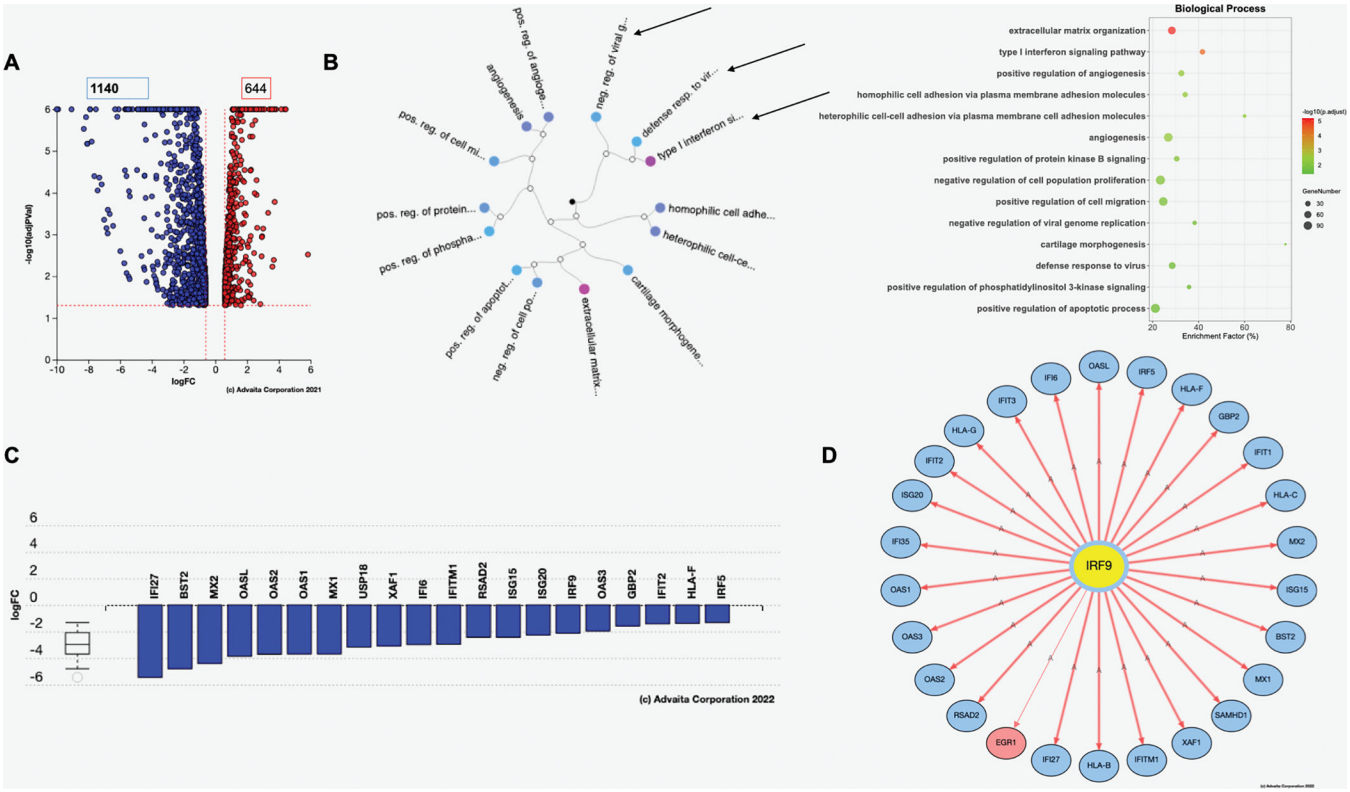

Figure 8. Knock-out of Twist1 is associated with decreased ISG expression levels.

A. Volcano plot comparing wt Sw71 cells and TWKO cells. 1140 genes were down regulated and 644 were upregulated in TWKO cells. Genes with FDR-adjusted p-value < 0.05 and absolute log2-foldchange > 0.6 were considered differentially expressed.

B. Dendrogram of main biological processes affected by Twist1 KO. Analysis was performed using High-specificity pruning. One of the top biological processes associated with the loss of Twist1 is Type I interferon signaling.

C. Differentially expressed genes in Type I interferon signaling pathway comparing TWKO cells and wt Sw71 cells. Note that all the differentially expressed genes were downregulated.

D. Network analysis of differentially expressed genes in the Type I interferon signaling pathway comparing TWKO cells and wt Sw71 cells. Note that these differentially expressed genes are all regulated by IRF9.

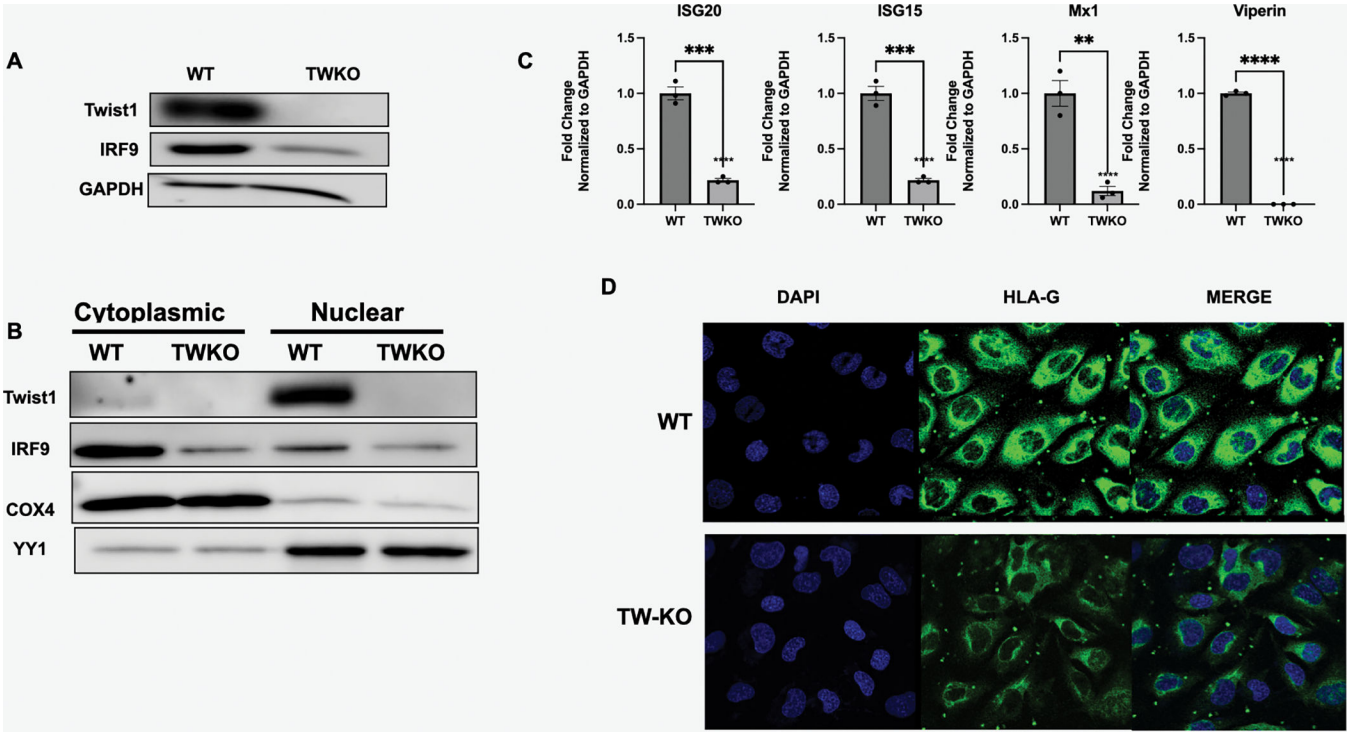

Figure 9. Inhibition of IRF9 basal expression in TWKO cells.

A. Expression of Twist1 and IRF9 were determined by Western blot analysis in wt Sw71 cells and TWKO cells. Not reduction in IRF9 levels in TWKO cells. Representative imagine of n=3 independent experiments.

B. Cellular location of Twist1 and IRF9 were determined by nuclear/cytoplasmic fractionation. Twist1 is mainly localized in the nuclei of wt cells and is absent in TWKO cells. IRF9 is mainly localized in the cytoplasm of wt cells and reduced TWKO cells. COX4 and YY1 are makers for the purity of the fractions. COX4 cytoplasmic, YY1 nucleus. Representative imagines of n=3 independent experiments

C. ISG20, ISG15, Mx1 and Viperin were quantified in wt Sw71 cells and TWKO cells by PCR. Note significant decrease in TWKO cells compared to wt Sw71 cells. N=3 independent experiments. **=p>0.001; ***=p.005; ****=p>0.0001

D. HLA-G expression in wt Sw71 cells and TWKO cells by immunofluorescence. HLAG expression is a characteristic of EVTs and it is highly expressed in wt Sw71 cells but is highly reduced in TWKO cells. Representative imagines of n=3 independent experiments

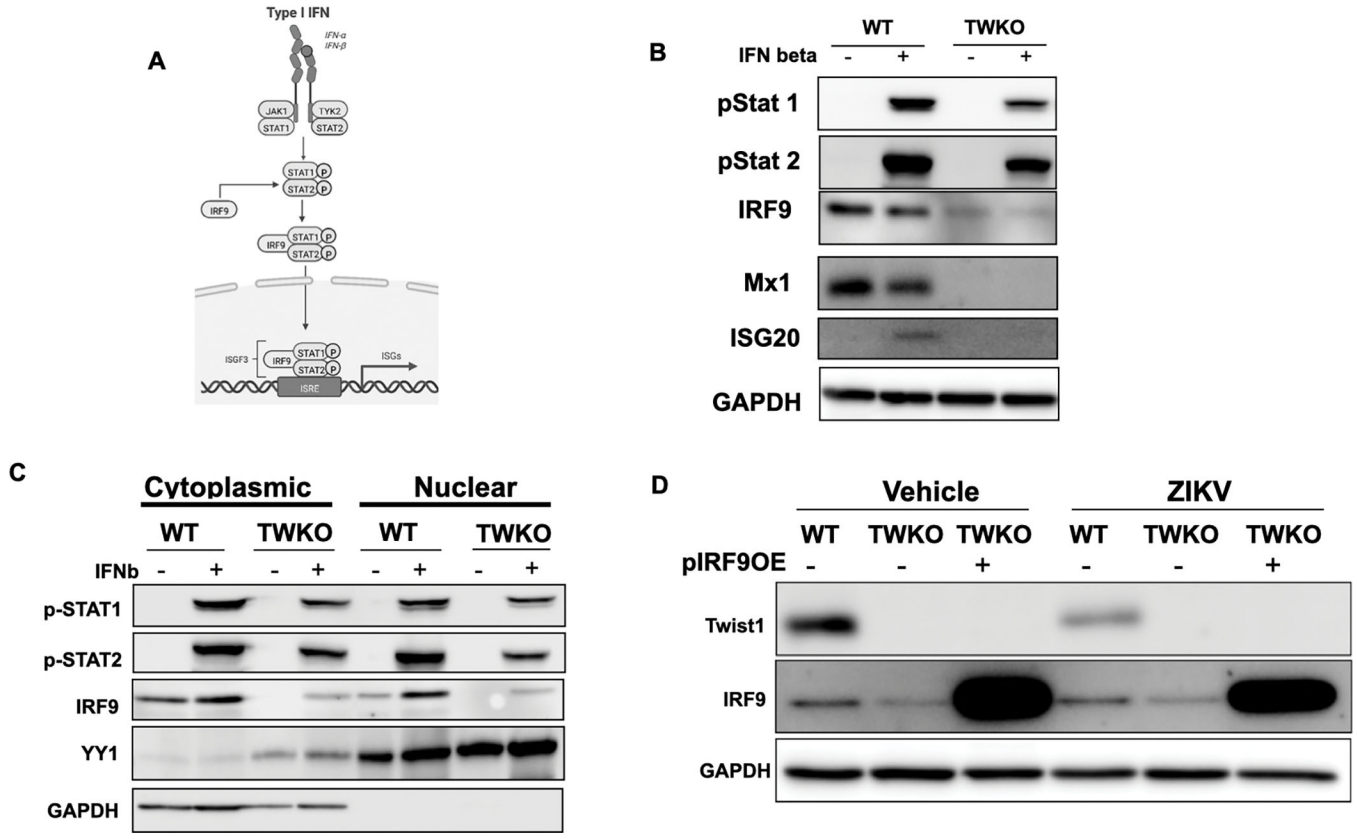

Figure 10. Integrity of the type I IFNβ canonical pathway

A. Schematic representation of the canonical IFNβ pathway.

B. Wild-type Sw71 cells and TWKO cells were treated Treatment with IFNβ and activation of canonical IFNβ pathway was determined by western blot. Note the phosphorylation of STAT1 and STAT2 in both wt and TWKO cells but IRF9, Mx1 and ISG20 were only detected in wild-type Sw71 cells. Representative imagine of n=3 independent experiments.

C. Nuclear and cytoplasmic fractionation in wild-type Sw71 cells and TWKO cells following IFNβ treatment. Note nuclear translocation of pSTAT1 and pSTAT2 in both wild-type Sw71 cells and TWKO cells but nuclear IRF9 is only detected in wt Sw71 cell following IFNβ treatment. Representative imagine of n=3 independent experiments.

D. Overexpression of IRF9 in wild-type Sw71 cells and TWKO cells infected with ZIKV. Representative imagines of n=3 independent experiments

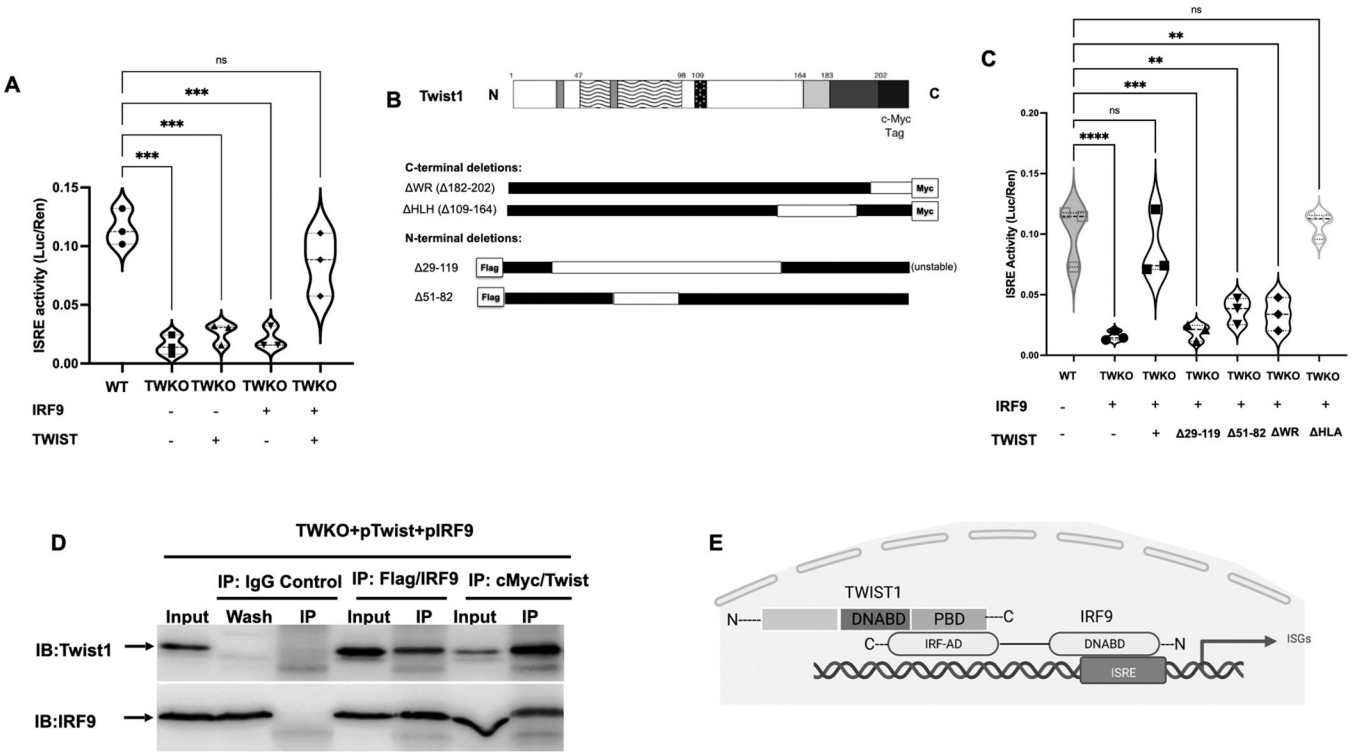

Figure 11. ISRE transcriptional activity in wt Sw71 cells and TWKO cells.

A. ISRE/Luc/Ren reporter system was transfected in wild-type Sw71 cells and TWKO cells together with IRF9 and/or Twist1 as indicated. Note significant decrease in ISRE activity in TWKO cells, which was rescued with co-transfection of IRF9 and Twist1. n=3 independent experiments in triplicates. ***=p.005

B. Schematic illustration of Twist1 protein and the deletions used to identify the domain required for binding to IRF9. Twist1 N-terminal deletion mutants have Flag tag and C-terminal deletions have Myc tag.

C. ISRE activity was measured in Twist1-KO cells transfected with IRF9 and different Twist1 constructs as indicated. Transcriptional activity is observed following co-transfection with IRF9 and Twist. Deletions at the N-terminal and the WR domain but not at the HLH domain is associated with loss of transcriptional activity. Wt cells are used as positive control. n= 3 independent experiments done in triplicate. **=p>0.001; ***=p.005, ****=p>0.0001

D. TWKO cells were co-transfected with Twist and IRF9. Whole-cell lysates were used to immunoprecipitate the corresponding tag on Twist1 and IRF9 and IP complexes were probed to detect presence of Twist and IRF9. IgG was used as control for all IPs. Representative data of three independent experiments.

E. Proposed model for Twist1 and IRF9 interaction. See text for details.

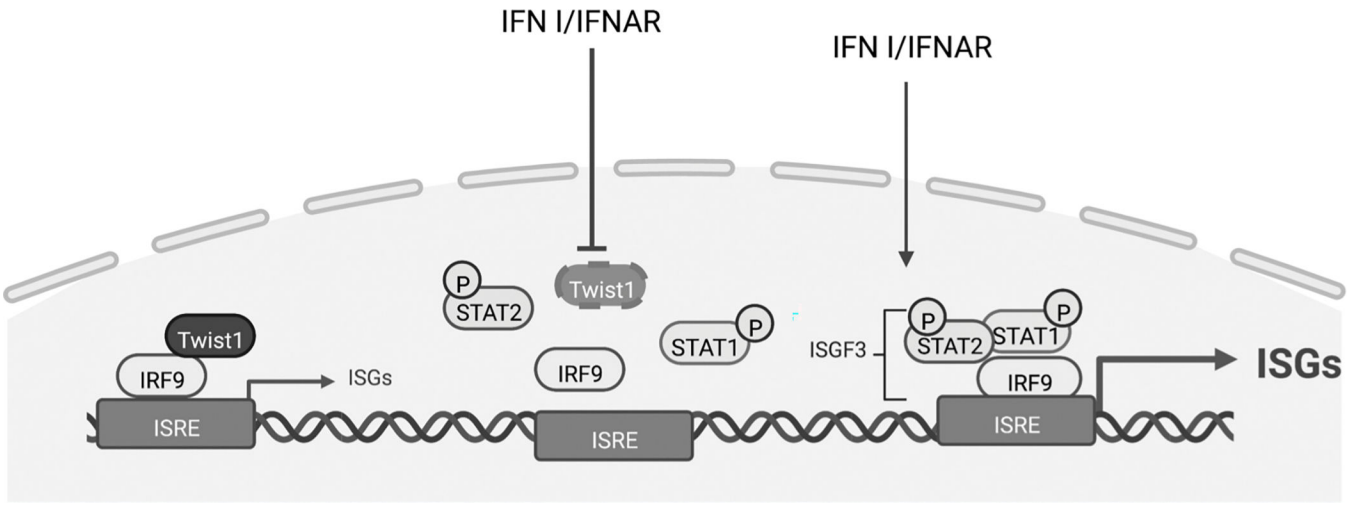

Fig. 12. Twist/IRF9 interaction maintains basal ISG expression.

Protein-protein interaction between Twist1 and IRF9 maintains provides early protection against viral infections. Activation of the IFNAR pathway leads to Twist degradation and release of IRF9, allowing the interaction with pSTAT1 and pSTAT2 and the formation of the ISGF3 complex.